1056 *Inorg. Chem.* **2010**, *49*, 1056–1070
DOI: 10.1021/ic901967h

Inorganic Chemistry
Article

Third Row Transition Metal Hexafluorides, Extraordinary Oxidizers, and Lewis Acids: Electron Affinities, Fluoride Affinities, and Heats of Formation of WF_6, ReF_6, OsF_6, IrF_6, PtF_6, and AuF_6[†]

Raluca Craciun, Désireé Picone, Rebecca T. Long, Shenggang Li, and David A. Dixon*

Department of Chemistry, The University of Alabama, Shelby Hall, Box 870336, Tuscaloosa, Alabama 35487-0336

Kirk A. Peterson

Department of Chemistry, Washington State University, Pullman, Washington 99164-4630

Karl O. Christe

Loker Hydrocarbon Research Institute and Department of Chemistry, University of Southern California, University Park, Los Angeles, California 90089

Received October 5, 2009

High level electronic structure calculations were used to evaluate reliable, self-consistent thermochemical data sets for the third row transition metal hexafluorides. The electron affinities, heats of formation, first ($MF_6 \rightarrow MF_5 + F$) and average M−F bond dissociation energies, and fluoride affinities of MF_6 ($MF_6 + F^- \rightarrow MF_7^-$) and MF_5 ($MF_5 + F^- \rightarrow MF_6^-$) were calculated. The electron affinities which are a direct measure for the oxidizer strength increase monotonically from WF_6 to AuF_6, with PtF_6 and AuF_6 being extremely powerful oxidizers. The inclusion of spin orbit corrections is necessary to obtain the correct qualitative order for the electron affinities. The calculated electron affinities increase with increasing atomic number, are in good agreement with the available experimental values, and are as follows: WF_6 (3.15 eV), ReF_6 (4.58 eV), OsF_6 (5.92 eV), IrF_6 (5.99 eV), PtF_6 (7.09 eV), and AuF_6 (8.20 eV). A wide range of density functional theory exchange-correlation functionals were also evaluated, and only three gave satisfactory results. The corresponding pentafluorides are extremely strong Lewis acids, with OsF_5, IrF_5, PtF_5, and AuF_5 significantly exceeding the acidity of SbF_5. The optimized geometries of the corresponding MF_7^- anions for W through Ir are classical MF_7^- anions with M−F bonds; however, for PtF_7^- and AuF_7^- non-classical anions were found with a very weak external F−F bond between an MF_6^- fragment and a fluorine atom. These two anions are text book examples for "superhalogens" and can serve as F atom sources under very mild conditions, explaining the ability of PtF_6 to convert NF_3 to NF_4^+, ClF_5 to ClF_6^+, and Xe to XeF^+ and why Bartlett failed to observe $XePtF_6$ as the reaction product of the PtF_6/Xe reaction.

Introduction

There is substantial interest in the development of strong electron acceptors to synthesize novel molecules with unique bonding properties as such syntheses often require very strong oxidizers. The first stable noble-gas compounds synthesized were the xenon fluorides[1,2] in the early 1960s. Bartlett first reported evidence for the xenon-containing compound, "$XePtF_6$",[3] which appears to be composed of $XeF^+PtF_6^-$, PtF_5, and $XeF^+Pt_2F_{11}^-$.[4] He used the metal hexafluoride PtF_6 in his reactions because of its ability to oxidize O_2, which has an ionization potential comparable to Xe, to form O_2^+ salts.[5] Bartlett[6,7] estimated that the electron affinities of the metal hexafluorides with the metal in the

[†] This paper is dedicated to the memory of Neil Bartlett.

*To whom correspondence should be addressed. E-mail: dadixon@bama.ua.edu.

(1) Bartlett, N.; Sladky, F. O. The Chemistry of Krypton, Xenon and Radon. In *Comprehensive Inorganic Chemistry*; Bailar, J. C., Jr., Emeléus, H. J., Nyholm, R., Trotman-Dickenson, A. F., Eds.; Pergamon Press: Oxford, U.K., 1973; Vol. *1*, pp 213−330.
(2) Malm, J. G.; Selig, H.; Jortner, J.; Rice, S .A. *Chem. Rev.* **1965**, *65*, 199–236.
(3) Bartlett, N. *Proc. Chem. Soc.* **1962**, 218.
(4) Graham, L.; Gaudejus, O.; Jha, N. K.; Bartlett, N. *Coord. Chem. Rev.* **2000**, *197*, 321–334.
(5) Bartlett, N.; Lohmann, D. H. *Proc. Chem. Soc.* **1962**, 115.
(6) Bartlett, N; Beaton, S. P.; Jha, N. K. *Chem. Commun.* **1966**, *6*, 169.
(7) Bartlett, N. *Angew. Chem., Int. Ed. Engl.* **1968**, *7*, 433.

 Published on Web 01/07/2010

Table 1. MF_6 Electron Affinities in eV

molecule	calculated[a]	experiment	reactivity estimate[f]	other calculated
WF_6	3.16	3.50 ± 0.1,[b] $3.36^{+0.4}_{-0.2}$[c]	*> 3.0*	3.34,[g] 3.85[h]
ReF_6	4.58	> 3.8[d]	> 3.90	4.50, [g] 4.8[i]
OsF_6	5.92	5.93 ± 0.28[e]	*> 4.7*	5.55, [g] 6.0[i]
IrF_6	5.99	6.50 ± 0.38[e]	> 5.46	5.34, [g] 7.2[i]
PtF_6	7.09	7.00 ± 0.35[e]	> 6.76	6.36,[g] 7.4[i], 6.95,[j] 6.78[k]
AuF_6	8.20		*> 7.6*	8.1,[i] 9.56 [l]

[a] Final calculated value this work. [b] Reference 8. [c] Reference 9. [d] Reference 86. [e] Reference 10. [f] References 6 and 7. Values in italics obtained from data in reference 7 using the estimate from this reference of a change in atomic number of 1 corresponds to a change of ~20 kcal/mol in the electron affinity. [g] DFT/BP86/TZP+DZP. Reference 41. [h] CI-SD+Q. Reference 39. [i] DV-Xα. Reference 37. From calculated EAs relative to 3.5 eV for WF_6. [j] CCSD(T)/ TZP+DZP. Reference 42, 43, 44. [k] B3LYP/ TZP+DZP. Reference 42. [l] CI-SD+Q. Reference 40.

formal +6 oxidation state (starting from WF_6) would increase across the row by ~20 kcal/mol from molecule to molecule. He proposed that EA(ReF_6) > 90 kcal/mol, EA(IrF_6) > 125 kcal/mol, EA(PtF_6) > 156 kcal/mol, and EA(AuF_6) > 176 kcal/mol (see Table 1) on the basis of their reactivity studies with reagents of different ionization potentials. On his scale, WF_6 would thus have an EA of ~70 kcal/mol (3.04 eV).

About a decade later, George and Beauchamp[8] used ion cyclotron resonance spectroscopy (ICR) to measure the electron affinity of WF_6 using bracketing techniques. Their value of 3.5 eV supports Bartlett's prediction that WF_6 is the poorest oxidizer among the third row hexafluorides. A value of $3.36^{+0.4}_{-0.2}$ eV was later derived from studies of the ion chemistry of WF_6, WF_6^-, and WF_7^-.[9] The latter ion molecule reaction bracketing studies showed that EA(WF_6) was between EA(Br) = 3.36 eV and EA(F) = 3.40 eV. The lower limit of 3.16 eV was due to the inclusion of the effects of internal and translational energy on the overall reaction energy. Sidorov and co-workers[10] used high temperature Knudsen cell mass spectrometry to obtain the electron affinities of OsF_6, IrF_6, and PtF_6 as shown in Table 1.

It is clear that the third row metal hexafluorides have some of the highest known electron affinities of stable, neutral molecules. They also serve as a set of molecules to probe interesting electronic structure effects. Using formal oxidation state arguments, the MF_6 molecules can be considered to be an M^{6+} ion surrounded by six F^- in an approximate octahedral ligand field. This means that one is filling the t_{2g} orbitals (d_{xy}, d_{xz}, d_{yz}) as the atomic number increases from W to Au (See Supporting Information). This resembles the filling of the p orbitals in main group compounds. As noted early for the MF_6 compounds, the partially occupied d orbitals in such high symmetry species can lead to Jahn−Teller distortions. Moffitt and co-workers[11] first explained the UV−visible absorption spectra of ReF_6, OsF_6, IrF_6, and PtF_6 and showed that the Jahn−Teller effect may be present as a vibronic coupling as well as a symmetry distortion. The subsequent experimental vibrational spectra[12−17] of ReF_6, OsF_6, and PtF_6 supported the conclusions of Moffitt and co-workers. The results raised questions about the role of spin−orbit (relativistic) effects on the properties of these compounds.

Seppelt has reviewed the structures and properties of the metal hexafluorides.[18] Electron diffraction measurements[19] of MF_6 molecular structures (M = W, Re, Os, Ir, and Pt) have been made by Hedberg and co-workers. These measurements show that the structures are all essentially octahedral under the experimental conditions. The M−F bond lengths for the first three members of the series are approximately the same, and the M−F bond lengths for the last two are longer. The same trend in the bond lengths was observed by Seppelt and co-workers[20] in their single-crystal structure determination study of second and third row transition metal hexafluorides. Seppelt and co-workers[21] have also discussed the stability of the octahedral structure of WF_6 relative to the regular or distorted trigonal prismatic structure and predicted the O_h structure to be more stable than the D_{3h} structure by 11 kcal/mol at the density functional theory (DFT)[22] level with the B3LYP[23,24] exchange-correlation functional. Bartlett and co-workers[25] measured the M−F interatomic distances in $LiMF_6$ and Li_2MF_6 salts of the second and third row transition series by using synchrotron X-ray powder diffraction following the initial work of the Bartlett group[26] on the synthesis[27] and structural characterization of $LiMF_6$ salts for M = Pt and Au.

There are only a few experimental studies of the heats of formation of the third row transition metal hexafluorides[28] and no reliable theoretical predictions of this fundamental thermodynamic property. For WF_6, the first reported value of -422 ± 4 kcal/mol for $\Delta H_{f,298K}(WF_6)$ is from a solution

(8) George, P M.; Beauchamp, J. L. *Chem. Phys.* **1979**, *36*, 345.
(9) Viggiano, A. A.; Paulson, J. F.; Dale, F.; Henchman, M.; Adams, N. G.; Smith, D. *J. Phys. Chem.* **1985**, *89*, 2264.
(10) Korobov, M. V.; Kuznetsov, S. V.; Sidorov, L. N.; Shipachev, V. A.; Mit'kin, V. N. *Int. J. Mass. Spectrom. Ion Processes* **1989**, *87*, 13.
(11) Moffit, W.; Goodman, G. L.; Fred, M.; Weinstock, B. *Mol. Phys.* **1959**, *2*, 109.
(12) Weinstock, B.; Claassen, H. H. *J. Chem. Phys.* **1959**, *31*, 262.
(13) Weinstock, B.; Claassen, H. H.; Malm, J. G. *J. Chem. Phys.* **1960**, *32*, 181.
(14) Weinstock, B.; Claassen, H. H.; Chernick, C. L. *J. Chem. Phys.* **1963**, *38*, 1470.
(15) Weinstock, B.; Goodman, G. *Adv. Chem. Phys.* **1965**, *9*, 169.
(16) Claassen, H. H.; Selig, H. *Israel J. Chem.* **1969**, *7*, 499.
(17) Claassen, H. H.; Goodman, G. L.; Holloway, J. H.; Selig, H. *J. Chem. Phys.* **1970**, *53*, 341.
(18) (a) Molski, M. J.; Seppelt, K. *Dalton Trans.* **2009**, 3379. (b) Seppelt, K. *Acc. Chem. Res.* **2003**, *36*, 147.
(19) Richardson, A. D.; Hedberg, K.; Lucier, G. M. *Inorg. Chem.* **2000**, *39*, 2787.
(20) Drews, T.; Super, J.; Hagenbach, A.; Seppelt, K. *Inorg. Chem.* **2006**, *45*, 3782.
(21) Quiñones, G. S.; Hägele, G.; Seppelt, K. *Chem.—Eur. J.* **2004**, *10*, 4755.
(22) Parr, R. G.; Yang, M. *Density-Functional Theory of Atoms and Molecules*; Oxford University Press: New York, 1989.
(23) Becke, A. D. *J. Chem. Phys.* **1993**, *98*, 5648.
(24) Lee, C.; Yang, W.; Parr, R. G. *Phys. Rev. B* **1988**, *37*, 785.
(25) Graudejus, O.; Wilkinson, A. P.; Chacon, L. C.; Bartlett, N. *Inorg. Chem.* **2000**, *39*, 2794.
(26) Graudejus, O.; Elder, S. H.; Lucier, G. M.; Shen, C.; Bartlett, N. *Inor. Chem.* **1999**, *38*, 2503.
(27) Leary, K.; Bartlett, N. *J. Chem. Soc., Chem. Commun.* **1972**, 903.
(28) Chase, M. W. Jr. NIST-JANAF Thermochemical Tables, 4th ed.; *J. Phys. Chem. Ref. Data* **1998**, Mono. 9, Suppl. 1.

calorimetry experiment.[29] Subsequent studies of tungsten combustion in fluorine in a bomb calorimeter yielded values of −411.5 ± 0.4 kcal/mol,[30] −411.7 ± 0.5 kcal/mol,[31] and −411.4 ± 0.2 kcal/mol.[32] For ReF_6, an estimated value of −322.6 ± 2.3 kcal/mol is available from hydrolysis measurements.[33] The heat of formation of OsF_6 is not known and that of IrF_6, estimated in 1929 as −130 kcal/mol[34] from the temperature rise during its preparation, is probably not reliable. The heat of formation of PtF_6 was determined by Knudsen-cell mass spectrometry to be −161.6 ± 6.7 kcal/mol[35] and calculated from calorimetric literature data to be −160.6 ± 1.5 kcal/mol.[36]

A number of theoretical studies have predicted the electron affinities (EA) of the metal hexafluorides. Gutsev and Boldyrev[37,38] used the non-relativistic Xα method to calculate electron affinities for the MF_6 molecules relative to the experimental value[8] of 3.50 eV for WF_6. Miyoshi and co-workers[39,40] used modest level configuration interaction (CI) calculations to predict the electron affinities of WF_6 and AuF_6. The first and second electron affinities of the 5d metal hexafluorides and hexachlorides have been predicted by Macgregor and Moock using DFT.[41] More recently, Wesendrup and Schwerdtfeger[42] used different levels of theory up to the coupled cluster theory (CCSD(T)) level to predict the structure and electron affinities of molecular platinum fluorides PtF_{2n} (n = 1−4). The structure of AuF_6 as well as its electron affinity (and that of PtF_6) have been investigated at different levels of theory by Riedel and Kaupp.[43] PtF_6 has been studied, in part, to predict the effect of including relativistic effects in the treatment of its geometry.[44−46]

Molecular fluoride affinities provide an estimate of the Lewis acid strength of a given species.[47] Bartlett[7] suggested, on the basis of the reactions of third row hexafluorides with ONF, that the fluoride affinity decreases along the MF_6 series in contrast to the increase in electron affinity. The fluoride affinity of WF_6 was measured in an ion cyclotron resonance bracketing study as 69 ± 5 kcal/mol (3.0 ± 0.2 eV); this value is based on the observation that SiF_5^- transfers F^- to WF_6 but BF_4^- does not.[8]

We describe the results of our high level electronic structure calculations at the CCSD(T) level of the structures, electron affinities, heats of formation, first ($MF_6 \rightarrow MF_5 + F$) and average M−F bond dissociation energies, and fluoride affinities ($MF_6 + F^- \rightarrow MF_7^-$) of MF_6 for M = W, Re, Os, Ir, Pt, and Au. We also report the fluoride affinities of MF_5 as these can be directly calculated from our data. The electron affinities can be used in the development of a quantitative scale of the strength of very strong oxidizers. The electron affinity and the fluoride affinity often compete with each other so good values for both are required to design the optimal oxidizing agent. In addition, we report on the ability of DFT to predict these energetic properties.

Computational Methods. Geometries and frequencies were calculated at the DFT level with a range of local,[48,49] gradient-corrected[24,50−57] and hybrid[23,24,58,59] exchange-correlation functionals including B3LYP (See Supporting Information). These calculations were performed with the augmented correlation consistent double-ζ (aug-cc-pVDZ) basis set for F[60] and the aug-cc-pVDZ-PP basis sets with accompanying small-core relativistic pseudopotentials for the transition metal atoms;[61] we label the combined basis set as aN-PP with N = D, T, Q. For all of the calculations described below, the zero point energy corrections and the temperature corrections from 0 to 298 K were obtained at the B3LYP/aT-PP level unless it was necessary to use the frequencies obtained with the BP86 functional.

Geometries were also optimized at the CCSD(T) level[62−65] with the aD-PP and aT-PP basis sets, and single point CCSD(T) energies were calculated with the aQ-PP basis set. The CCSD(T) energies could then be extrapolated to the complete basis set (CBS) limit by using a mixed Gaussian/exponential formula.[66] An additional electronic energy correction to the CCSD(T)/CBS valence energies is the core−valence correlation correction (ΔE_{CV}) calculated at the CCSD(T) level with the

(29) Myers, O. E.; Brady, A. P. *J. Phys. Chem.* **1960**, *64*, 591.
(30) O'Hare, P. A. G.; Hubbard, W. N. *J. Phys. Chem.* **1966**, *70*, 3353.
(31) Schroeder, J.; Sieben, F. J. *Chem. Ber.* **1970**, *103*, 76.
(32) Pervov, V. S.; Klyuev, L. I.; Gaisinskaya, O. M.; Medvedev, V. A.; Nikolaev, N. S. *Doklady Akademii Nauk SSSR* **1972**, *205*, 349.
(33) Burgess, J.; Fraser, C. J. W.; Peacock, R. D. *J. Chem. Soc., Dalton Trans.* **1973**, 501.
(34) Ruff, O.; Fischer, J. *Z. Anorg. Allg. Chem.* **1929**, *179*, 161.
(35) Korobov, M. V.; Nikulin, V. V.; Chilingarov, N. S.; Sidorov, L. N. *J. Chem. Thermodyn.* **1986**, *18*, 235.
(36) Nikitin, M. I.; Karpukhina, E. V. *Zh. Neorg. Khim.* **2007**, *52*, 531.
(37) Gutsev, G. L.; Boldyrev, A. I. *Chem. Phys. Lett.* **1983**, *101*, 441.
(38) Gutsev, G. L.; Levin, A. A. *Chem. Phys.* **1980**, *51*, 459.
(39) Miyoshi, E.; Sakai, Y.; Murakami, A.; Iwaki, H.; Terashima, H.; Shoda, T.; Kawaguchi, T. *J. Chem. Phys.* **1988**, *89*, 4193.
(40) Miyoshi, E.; Sakai, Y. *J. Chem. Phys.* **1988**, *89*, 7363.
(41) Macgregor, S. A; Moock, K. H. *Inorg. Chem.* **1998**, *37*, 3284.
(42) Wesendrup, R.; Schwerdtfeger, P. *Inorg. Chem.* **2001**, *40*, 3351.
(43) Riedel, S.; Kaupp, M. *Inorg. Chem.* **2006**, *45*, 1228.
(44) Riedel, S. *J. Fluorine Chem.* **2007**, *128*, 938.
(45) Alvarez-Thon, L.; David, J.; Arratia-Perez, R.; Seppelt, K. *Phys. Rev. A* **2008**, *77*, 034502.
(46) David, J.; Fuentealba, P.; Restrepo, A. *Chem. Phys. Lett.* **2008**, *457*, 42.
(47) Christe, K. O.; Dixon, D. A.; McLemore, W. W.; Wilson; Sheehy, J.; Boatz, J. A. *J. Fluorine Chem.* **2000**, *101*, 151. *Chem. Eng. News*, pp. 48−49, March 3, **2003**.
(48) Slater, J. C. *Quantum Theory of Molecules and Solids*; McGraw-Hill: New York, 1974; Vol. *4*.
(49) Vosko, S. H.; Wilk, L.; Nusair, M. *Can. J. Phys* **1980**, *58*, 1200.
(50) Becke, A. D. *Phys. Rev. A* **1988**, *38*, 3098.
(51) Perdew, J. P. *Phys. Rev. B* **1986**, *33*, 8822.
(52) Perdew, J. P.; Wang, Y. *Phys. Rev. B* **1991**, *45*, 13244.
(53) Burke, K.; Perdew, J. P. Wang. Y. In *Electronic Density Functional Theory: Recent Progress and New Directions*; Dobson, J. F., Vignale, G., Das, M. P., Eds.; Plenum: New York, 1998; p 81.
(54) Perdew, J. P.; Burke, K.; Ernzerhof, M. *Phys. Rev. Lett.* **1996**, *77*, 3865.
(55) Perdew, J. P.; Burke, K.; Ernzerhof, M. *Phys. Rev. Lett.* **1997**, *78*, 1396.
(56) Tao, J. M.; Perdew, J. P.; Staroverov, V. N.; Scuseria, G. E. *Phys. Rev. Lett.* **2003**, *91*, 146401.
(57) Hamprecht, F. A.; Cohen, A. J.; Tozer, D. J.; Handy, N. C. *J. Chem. Phys.* **1998**, *109*, 6264.
(58) Adamo, C.; Barone, V. *Chem. Phys. Lett.* **1997**, *274*, 242.
(59) Handy, N. C.; Cohen, A. J. *Mol. Phys.* **2001**, *99*, 403.
(60) Kendall, R. A.; Dunning, T. H., Jr.; Harrison, R. J. *J. Chem. Phys.* **1994**, *96*, 6796.
(61) Figgen, D.; Peterson, K. A.; Dolg, M.; Stoll, H. *J. Chem. Phys.* **2009**, *130*, 164108.
(62) Purvis, G. D., III; Bartlett, R. J. *J. Chem. Phys.* **1982**, *76*, 1910.
(63) Raghavachari, K.; Truck, G. W.; Pople, J. A.; Head-Gordon, M. *Chem. Phys. Lett.* **1989**, *157*, 479.
(64) Watts, J. D.; Gauss, J.; Bartlett, R. J. *J. Chem.. Phys.* **1993**, *98*, 8718.
(65) Bartlett, R. J.; Musial, M. *Rev. Mod. Phys.* **2007**, *79*, 291.
(66) Peterson, K. A.; Woon, D. E.; Dunning, T. H., Jr. *J. Chem. Phys.* **1994**, *100*, 7410.

aug-cc-pwCVTZ basis set for F[67,68] and the aug-cc-pwCVTZ-PP basis set for the transition metal atoms (denoted as awCVTZ). Scalar relativistic corrections on the F atoms and corrections for any errors in the metal pseudopotentials for the electron affinities (EAs) were obtained by taking the difference between the EA calculated at the Douglas−Kroll−Hess[69] level with the CCSD(T)-DK method and the aT-DK basis set[61,70,71] and the EA calculated at the CCSD(T)/aT-PP level (eq 1).

$$\Delta EA_{Rel} = EA(CCSD(T)\text{-}DK/aT\text{-}DK) - EA(CCSD(T)/aT\text{-}PP) \quad (1)$$

A separate estimate of just the pseudopotential error is described in the Supporting Information and is less than 2.5 kcal/mol (∼0.1 eV) for the electron affinities. One final correction that needs to be considered is that of spin orbit. Molecular spin orbit corrections were calculated at the BLYP/TZ2P level using the spin orbit approach and scalar two-component zero-order regular approximation (ZORA)[72] as implemented in the ADF 2008.01 program.[73] The spin orbit (SO) correction is taken as the difference between the ZORA and ZORA + SO values at a specific property. The electron affinity was thus calculated as the sum of different contributions (eq 2).

$$EA_{0K} = EA_{CBS} + \Delta EA_{ZPE} + \Delta EA_{CV} + \Delta EA_{Rel} + \Delta EA_{SO} \quad (2)$$

A similar equation was used to calculate the total atomization energies (TAEs), which are used to calculate the molecular heats of formation. In calculating the TAEs, we chose the low-lying atomic state with no SO splitting if possible, and used the experimental SO splittings otherwise.[74] The experimental atomic heats of formation at 0 K were taken from the JANAF Tables[28] for F and W and from the compilation of Wagman et al.[75] for the remaining metals (See Supporting Information). No error bars were reported for the latter values. The atomic heats of formation have also been given by Greenwood and Earnshaw,[76] and these can be used to help provide ranges for the heats of formation. The heat of formation of Os is not given at 0 K, so we estimated that its value is 0.2 kcal/mol lower than the 298 K value following the trends in the other metals. The above additive approach follows the general approach to the prediction of heats of formation developed at Washington State University, the Pacific Northwest National Laboratory, and The University of Alabama.[77]

Results and Discussion

Geometries of the Hexafluorides. Table 2 lists the metal−fluorine bond distances of the neutral hexafluorides and their anions optimized at the CCSD(T) levels with aT-PP basis set and at the ZORA and ZORA SO BLYP/TZ2P levels. The Cartesian coordinates, as well as the geometries optimized with the various DFT exchange correlation functionals and the CCSD(T)/aD-PP method, are given as Supporting Information. We explored a variety of structures (symmetries) and orbital combinations in our studies of the open shell molecules to obtain the ground state structures.

Qualitative Description of MF_6 Structures. Before describing the results of the calculations, we describe the types of structures and states that are expected. The 5d orbitals in an octahedral field will split into a t_{2g} set and an e_g set with the t_{2g} orbitals below the e_g orbitals. We assume a formal +6 oxidation state on the metal atoms and no spin orbit coupling for the following argument. Thus, one is filling the t_{2g} orbitals starting from WF_6 with no d electrons so WF_6 should have O_h symmetry. WF_6^- has one d electron and will undergo a Jahn−Teller distortion to D_{4h} or D_{3d} symmetry. Distortion to D_{4h} symmetry gives an e_g and a b_{2g} orbital from the t_{2g} orbitals. Occupancy of the b_{2g} orbital leads to a structure with 2 short and 4 long M−F bonds. Distortion to D_{3d} symmetry gives an e_g and an a_{1g} orbital from the t_{2g} orbitals. Occupancy of the a_{1g} orbital leads to a structure with 6 equivalent M−F bonds with angles that deviate only slightly from 90°. ReF_6 will have a structure similar to WF_6^-. In D_{4h} symmetry, ReF_6^- has two potential electron occupancies, a $(b_{2g})^2$ occupancy giving rise to a $^1A_{1g}$ state or an $(e_g)^2$ occupancy leading to a $^3A_{1g}$ state. Thus the lowest energy state depends on which of the e_g and b_{2g} orbitals lies the lowest. If the b_{2g} orbital lies the

(67) Woon, D. E.; Dunning, T. H., Jr. *J. Chem. Phys.* **1995**, *103*, 4572.
(68) Peterson, K. A.; Dunning, T. H., Jr. *J. Chem. Phys.* **2002**, *117*, 10548.
(69) (a) Douglas, M.; Kroll, N. M. *Ann. Phys.* **1974**, *82*, 89. (b) Hess, B. A. *Phys. Rev. A.* **1985**, *32*, 756. (c) Hess, B. A. *Phys. Rev. A.* **1986**, *33*, 3742.
(70) de Jong, W. A.; Harrison, R. J.; Dixon, D. A. *J. Chem. Phys.* **2001**, *114*, 48.
(71) EMSL basis set library: http://www.emsl.pnl.gov/forms/basisform.html
(72) (a) van Lenthe, E.; Ehlers, A. E.; Baerends, E. J. *J. Chem. Phys.* **1999**, *110*, 8943. (b) van Lenthe, E.; Baerends, E. J.; Snijders, J. G. *J. Chem. Phys.* **1993**, *99*, 4597. (c) van Lenthe, E.; Baerends, E. J.; Snijders, J. G. *J. Chem. Phys.* **1994**, *101*, 9783. (d) van Lenthe, E.; Snijders, J. G.; Baerends, E. J. *J. Chem. Phys.* **1994**, *105*, 6505. (e) van Lenthe, E.; van Leeuwen, R.; Baerends, E. J.; Snijders, J. G. *Int. J. Quantum Chem.* **1996**, *57*, 281.
(73) (a) te Velde, G.; Bickelhaupt, F.M.; van Gisbergen, S. J. A.; Fonseca Guerra, C.; Baerends, E.J.; Snijders, J.G.; Ziegler, T. *J. Comput. Chem.* **2001**, *22*, 931. (b) Fonseca Guerra, C.; Snijders, J.G.; te Velde, G.; Baerends, E.J. *Theor. Chem. Acc.* **1998**, *99*, 391. (c) *ADF2008.01*; SCM, Theoretical ChemistryVrije Universiteit: Amsterdam, The Netherlands, http://www.scm.com.
(74) Moore, C. E. *Atomic energy levels as derived from the analysis of optical spectra, Volume 1, H to V*; U.S. National Bureau of Standards Circular 467, U.S. Department of Commerce, National Technical Information Service, COM-72−50282: Washington, D.C., 1949.
(75) Wagman, D. D.; Evans, W. H.; Parker, V. B.; Schumm, R. H.; Halow, I.; Bailey, S. M.; Churney, K. L.; Nuttall, R. L. *J. Phys. Chem. Ref. Data*, **1982**, *11*, Supplement 2.
(76) Greenwood, N. N.; Earnshaw, A. *Chemistry of the Elements*; Pergamon Press: Oxford, 1984; (W, Chapter 23, p 1170; Re, Chapter 24, p 1214; Os, Chapter 25, p 1248; Ir, Chapter 26, p 1294; Pt, Chapter 27, p 1333; Au, Chapter 28, p 1368).
(77) (a) Feller, D.; Dixon, D. A. *J. Phys. Chem. A* **2000**, *104*, 3048. (b) Feller, D.; Dixon, D. A. *J. Chem. Phys.* **2001**, *115*, 3484. (c) Dixon, D. A.; Feller, D.; Peterson, K. A. *J. Chem. Phys.* **2001**, *115*, 2576. (d) Ruscic, B.; Wagner, A. F.; Harding, L. B.; Asher, R. L.; Feller, D.; Dixon, D. A.; Peterson, K. A.; Song, Y.; Qian, X.; Ng, C.; Liu, J.; Chen, W.; Schwenke, D. W. *J. Phys. Chem. A* **2002**, *106*, 2727. (e) Feller, D.; Dixon, D. A. *J. Phys. Chem. A* **2003**, *107*, 9641. (f) Dixon, D. A.; Feller, D.; Christe, K. O.; Wilson, W. W.; Vij, A.; Vij, V.; Jenkins, H. D. B.; Olson, R. M.; Gordon, M. S. *J. Am. Chem. Soc.* **2004**, *126*, 834. (g) Dixon, D. A.; Gutowski, M. *J. Phys. Chem. A* **2005**, *109*, 5129. (h) Pollack, L.; Windus, T. L.; de Jong, W. A.; Dixon, D. A. *J. Phys. Chem. A* **2005**, *109*, 6934. (i) Gutowski, K. E.; Dixon, D. A. *J. Phys. Chem. A* **2006**, *110*, 12044. (j) Matus, M. H.; Anderson, K. D.; Camaioni, D. M.; Autrey, S. T.; Dixon, D. A. *J. Phys. Chem. A* **2007**, *111*, 4411. (k) Feller, D.; Peterson, K. A.; Dixon, D. A. *J. Chem. Phys.* **2008**, 129 204015.

Table 2. Optimized Metal−Fluorine Bond Lengths (Å) and Bond Angles (deg) at the CCSD(T) Level with the aT-PP Basis Set and at the ADF ZORA BLYP Level with the TZ2P Basis Set

molecule	state/sym	CCSD(T)/aT-PP	state/sym ZORA	ZORA TZ2P	sym ZORA-SO	ZORA S−O TZ2P	expt
WF_6	$^1A_{1g}/O_h$	1.835	$^1A_{1g}/O_h$	1.889	O_h	1.887	1.825[a],1.829[b],1.826[c]
WF_6^-	$^2B_{2g}/D_{4h}$	1.865 (×2),1.921 (×4)	$^2A_{1g}/D_{3d}$	1.951, 92.7°	D_{4h}	1.970 (×2), 1.943 (×4)	
WF_6^-	$^2A_{1g}/D_{3d}$	1.902, 92.7°			D_{3d}	1.950, 92.5°	
ReF_6	$^2B_{2g}/D_{4h}$	1.802 (×2), 1.844 (×4)	$^2A_{1g}/D_{3d}$	1.885, 91.8°	D_{4h}	1.899 (×2), 1.878 (×4)	1.829[b]
ReF_6	$^2A_{1g}/D_{3d}$	1.830, 91.8°			D_{3d}	1.883, 91.0°	
ReF_6^-	$^3A_{1g}/D_{4h}$	1.927 (×2), 1.873 (×4)	$^3A_{1g}/D_{3d}$	1.942, 91.6°	D_{4h}	1.928 (×2), 1.951 (×4)	1.863[d]
ReF_6^-	$^3A_{1g}/D_{3d}$	1.891, 90.8°			D_{3d}	1.941, 90.6°	
OsF_6	$^3A_{1g}/D_{4h}$	1.856 (×2), 1.816 (×4)	$^3A_{1g}/O_h$	1.887	D_{4h}	1.877 (×2), 1.892 (×4)	1.827[a], 1.828[b]
OsF_6	$^3A_{1g}/D_{3d}$	1.829, 90.7°	$^3A_{1g}/D_{3d}$	1.886, 91.2°	D_{3d}	1.885, 90.4°	
OsF_6^-	$^4A_{1g}/O_h$	1.884	$^4A_{1g}/O_h$	1.938	O_h	1.939	1.872[e], 1.879[e]
IrF_6	$^4A_{1g}/O_h$	1.832	$^4A_{1g}/O_h$	1.893	O_h	1.894	1.839[b]
IrF_6^-	$^3A_{1g}/D_{4h}$	1.849 (×2), 1.897 (×4)	$^3A_{1g}/D_{3d}$	1.941, 91.1°	D_{4h}	1.952 (×2), 1.938 (×4)	1.879[e], 1.875[f]
IrF_6^-	$^3A_{1g}/D_{3d}$	1.881, 91.3°			D_{3d}	1.940, 90.4°	
PtF_6	$^3A_{1g}/D_{4h}$	1.823 (×2), 1.856 (×4)	$^3A_{1g}/O_h$	1.911	D_{4h}	1.915 (×2), 1.909 (×4)	1.852[b]
PtF_6	$^3A_{1g}/D_{3d}$	1.845, 90.1°			D_{3d}	1.908, 90.2°	
PtF_6^-	$^2B_{2g}/D_{4h}$	1.917 (×2), 1.869 (×4)	$^2B_{2g}/O_h$	1.951	O_h	1.952	1.887[e]
PtF_6^-	$^2A_{1g}/D_{3d}$	1.884, 90.6°					
AuF_6	$^2B_{2g}/D_{4h}$	1.897 (×2), 1.878 (×4)	$^2B_{2g}/O_h$	1.937	O_h	1.936	
AuF_6	$^2A_{1g}/D_{3d}$	1.870, 90.2°	$^2A_{1g}/D_{3d}$	1.938, 90.2°	D_{3d}	1.934, 90.1°	
AuF_6^-	$^1A_{1g}/O_h$	1.899	$^1A_{1g}/O_h$	1.966	O_h	1.967	1.899[c], 1.874[e], 1.861[g], 1.890[h]

[a] Reference 78. [b] Reference 19. [c] Reference 20. [d] Reference 79. [e] Reference 25. [f] Reference 80. [g] Reference 83. [h] Reference 81

lowest, then the $^1A_{1g}$ state should look like that of ReF_6 in terms of the geometry; if the $^3A_{1g}$ state is formed from the $(e_g)^2$ occupancy, then there should be 4 short and 2 long bonds. OsF_6 would be expected to exhibit the same type of behavior as ReF_6^-. In the distorted D_{3d} symmetry structure, the $(e_g)^2$ occupancy gives rise to a $^3A_{1g}$ state as well. For OsF_6^- and IrF_6, there are three d electrons so there is no need for a Jahn−Teller distortion as the $(t_{2g})^3$ electron configuration leads to the $^4A_{1g}$ high spin state in O_h symmetry. IrF_6^- and PtF_6 can be described by following the same considerations as for the triplet states in ReF_6^- or OsF_6. With four d electrons in D_{4h} symmetry, if the e_g orbital lies the lowest, then the state is $^1A_{1g}$ from the $(e_g)^4$ occupancy with 4 short bonds and 2 long bonds. If the b_{2g} orbital lies the lowest, then the occupancy is $(b_{2g})^2(e_g)^2$ leading to a $^3A_{1g}$ state with 2 short bonds and 4 long bonds. In D_{3d} symmetry, there is the possibility of the $(a_{1g})^2(e_g)^2$ occupancy leading to a $^3A_{1g}$ state or of $(e_g)^4$ occupancy leading to a $^1A_{1g}$ state. With five d electrons, there is one hole so the electron configuration in D_{4h} symmetry is $(e_g)^4(b_{2g})^1$ for a $^2B_{2g}$ state for PtF_6^- and AuF_6 with 4 short bonds and 2 long bonds. In D_{3d} symmetry, the electron configuration is $(e_g)^4(a_{1g})^1$ for a $^2A_{1g}$ state. AuF_6^- has six d electrons so the electron occupancy is $(t_{2g})^6$ with O_h symmetry. A consequence of this analysis is that the D_{4h} structures should have two different M−F bond distances whereas the D_{3d} structures will have only one M−F bond distance just as in the O_h symmetry structure. If the three D_{4h}, D_{3d}, and O_h structures are all close in energy, it will be extremely difficult experimentally in a structural determination to observe any structure that does not have approximate O_h symmetry. Contributions of the different corrections to the relative energy difference between the D_{4h} and D_{3d} structures are given in the Supporting Information. The geometry discussion below focuses on the CCSD(T)/aT-PP structures and energies unless noted.

WF_6. The calculated W−F bond distance for WF_6 (O_h) of 1.835 Å is in good agreement with those reported by Marx et al.[78] using neutron diffraction (1.825 Å), by Richardson et al.[19] using electron diffraction (r_g = 1.829(2) Å), and by Seppelt[20] in a single crystal structure determination (average of 1.826 Å). The previously reported values of 1.853 Å (Hartree−Fock) and 1.881 Å (single + double + Q correction CI (CI-SD+Q))[39] and of 1.886 Å (LDA/TZP/DFT[73])[41] are too long.

WF_6^- and ReF_6. In the D_{4h} structure with the b_{2g} orbital below the e_g orbital, WF_6^- and ReF_6 have two short axial bonds and four long equatorial bonds differing by 0.056 Å and 0.042 Å, respectively, with an average of 1.903 Å for r(W−F) and 1.830 Å for r(Re−F). The O_h structures, with the M−F bond distance calculated as the average of the bonds in the D_{4h} structures, were found to be no more than 1 kcal/mol higher in energy than the D_{4h} structures for both WF_6^- and ReF_6. The W−F bond length in the D_{3d} structure, which has essentially the same energy as the D_{4h} structure at the CCSD(T)/CBS level, is 1.902 Å.

We performed ZORA and ZORA-SO calculations to examine the effects of spin orbit coupling. For all MF_6 and MF_6^-, ZORA predicted an O_h or D_{3d} geometry to be the lowest energy structure. ZORA-SO predicted that WF_6^- distorts to a D_{4h} geometry with 2 long and 4 short bond distances, which is the opposite bonding pattern expected from simple orbital arguments without spin orbit. The D_{3d} structure for WF_6^- is only 0.59 kcal/mol higher in energy than the D_{4h} structure at ZORA-SO. When all of the energy contributions are combined, the D_{3d} structure for WF_6^- is only 0.5 kcal/mol above the D_{4h} structure (see Figure 1 for the state splittings). The ZORA-SO bond distance for WF_6 is 1.887 Å which is too long by about 0.06 Å as expected from other DFT calculations.[41] The spin orbit effect on the bond distance is a few thousandths of an angstrom.

For ReF_6, the D_{3d} structure is predicted to be slightly above the D_{4h} structure at the CCSD(T)/CBS level. The

(78) Marx, R.; Seppelt, K.; Ibberson, R. M. *J. Chem. Phys.* **1996**, *104*, 7658.

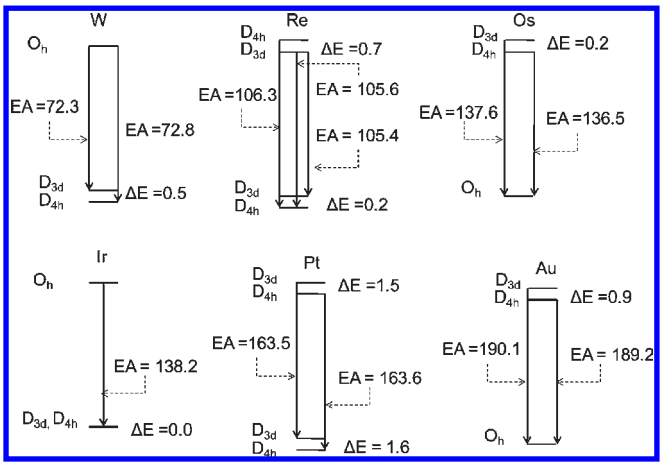

Figure 1. Schematic energy level diagram for use in predicting the molecular electron affinities for the MF_6 (in kcal/mol).

structure of ReF_6 has been measured by electron diffraction[19] and the bond distance for an O_h structure is r_g = 1.829(2) Å. This is in excellent agreement with our calculated values of 1.830 Å for the average distance in the D_{4h} structure and of 1.830 Å for the D_{3d} structure. ZORA-SO predicted the D_{3d} structure for ReF_6 to be 0.23 kcal/mol more stable than the D_{4h} structure. The ZORA-SO calculations with the BLYP functional give bond lengths that are too long by 0.06 Å as compared to experiment. The longer Re−F distance at the ZORA-SO level is consistent with a smaller difference between the long and short Re−F bond distances. ReF_6 may exhibit a Jahn−Teller distortion from the O_h structure as observed in its vibrational spectra.[12,15] The CCSD(T)/CBS energy difference and the spin−orbit correction essentially cancel for the energy difference between the D_{4h} and D_{3d} structures of ReF_6 so that the difference of the zero point energies, which favors the D_{3d} structure, is the most important leading to the D_{3d} structure being more stable than the D_{4h} structure by 0.7 kcal/mol.

ReF_6^- and OsF_6. The $^3A_{1g}/D_{4h}$ state is predicted to be the ground state for both ReF_6^- and OsF_6 with the $^1A_{1g}/D_{4h}$ state 25.8 and 23.6 kcal/mol, respectively, higher in energy. Both ReF_6^- and OsF_6 have two long axial bonds and four short equatorial bonds with differences less than 0.05 Å and an average of 1.891 Å for Re−F and 1.830 Å for Os−F. Marx et al.[78] reported an average distance of 1.827 Å for the Os−F bond in OsF_6 with the axial bonds longer by 0.018 Å than the equatorial bonds using neutron diffraction. The gas phase electron diffraction value[19] for OsF_6 is r_g = 1.828(2) Å as compared to our average value of 1.829 Å. The X-ray crystal structure value of r(Os−F) = 1.827 Å is also in good agreement.[78] As in the case of WF_6^- and ReF_6, the O_h geometries are less than 1 kcal/mol above the D_{4h} structure. The D_{3d} structure for ReF_6^- is 1.04 kcal/mol higher than the D_{4h} structure at the CCSD(T)/CBS level but the difference in zero point energies essentially cancels this value, and the D_{3d} structure is only 0.2 kcal/mol above the D_{4h} structure when all of the energy corrections are included. The Re−F distance in $CsReF_6$ was determined by X-ray crystallography[79] to be 1.863(4) Å, which is, surprisingly, almost 0.03 Å shorter than the calculated average value for the D_{4h} structure of 1.891 Å or the bond distance in the D_{3d} structure of 1.891 Å. The ZORA-SO D_{4h} structure for OsF_6 with 2 short and 4 long bond distances is only 0.15 kcal/mol higher in energy than the D_{3d} structure. The final result with all corrections is that the D_{4h} structure is 0.2 kcal/mol lower in energy than the D_{3d} structure for OsF_6.

OsF_6^- and IrF_6. Both OsF_6^- and IrF_6 have O_h symmetry. The calculated Os−F bond distance of 1.884 Å is close to the value of 1.8727 Å reported for the anion in the synchrotron X-ray powder diffraction study.[25] An X-ray powder diffraction study gives an Os−F bond length of 1.872(7) Å, and the single crystal structure of $LiOsF_6$ gives r(Os−F) = 1.879(4) Å.[25] The calculated Ir−F bond distance at 1.832 Å is in excellent agreement with the electron diffraction value of 1.839 Å.[19] Again, the DFT value of 1.928 Å reported by Macgregor and Moock[41] for Os−F in OsF_6^- is too long. Thus, comparing the average calculated M−F bond distances shows that there is a slight decrease from WF_6 to OsF_6 and a slight increase to IrF_6, but they are all essentially the same within 0.006 Å. The experimental gas phase values for r_g are essentially the same for WF_6, ReF_6, and OsF_6 and increase by about 0.01 Å for IrF_6. At the ZORA-SO level, IrF_6 is predicted to have O_h symmetry and a bond distance of 1.894 Å, which is too long by 0.055 Å as compared to experiment.

IrF_6^- and PtF_6. IrF_6^- and PtF_6 are predicted to have a $^3A_{1g}/D_{4h}$ ground state with two short and four long bonds with differences of less than 0.05 Å. The average bond distance for PtF_6 is 1.845 Å, in good agreement with the electron diffraction value[19] of r_g = 1.852(2) Å. The crystal structure[25] of $LiIrF_6$ determined by powder diffraction gives r(Ir−F) = 1.879(5) Å, and a single crystal structure[80] gives r(Ir−F) = 1.875(3) Å. The calculated value of 1.881 Å for the average Ir−F bond distance from the D_{4h} structure or the Ir−F distance in the D_{3d} structure is in very good agreement with the experimental values. The $^1A_{1g}/D_{4h}$ structures are 23.4 and 16.3 kcal/mol, respectively, for IrF_6^- and PtF_6, higher in energy than the $^3A_{1g}/D_{4h}$ geometry ground state. The O_h triplet structures are again only slightly higher than the D_{4h} geometries, and, for PtF_6, this difference is only 0.3 kcal/mol. The $^3A_{1g}/D_{3d}$ structure of IrF_6^- with a bond distance of 1.881 Å is 0.77 kcal/mol higher in energy than the $^3A_{1g}/D_{4h}$ ground state. At the ZORA-SO level, the D_{3d} and D_{4h} structures for IrF_6^- have the same energy. The ZPE difference favors the D_{3d} structure so when all energy corrections are included, the D_{3d} and D_{4h} structures for IrF_6^- have the same energy. At the ZORA-SO level, the PtF_6 structure has approximate O_h symmetry with the D_{3d} and D_{4h} structures equal in energy. The energies of the D_{4h} and D_{3d} structures are equal and <0.4 kcal/mol more stable than an O_h structure, consistent with previous four-component or ZORA-SO calculations with the BLYP functional.[45] In this case, the ZPE difference favors the D_{4h} structure, and the D_{4h} structure of PtF_6 is 1.5 kcal/mol more stable than the D_{3d} structure.

PtF_6^- and AuF_6. The D_{4h} structure has two long bonds and four short bonds with average values of 1.885 Å for PtF_6^- and 1.871 Å for AuF_6 with differences less than

(79) Hoskins, B. F.; Linden, A.; Mulvaney, Pc.C.; O'Donnell, T. A. *Inorg. Chim. Acta* **1984**, *88*, 217.

(80) Fitz, H.; Muller, B. G.; Graudejus, O.; Bartlett, N. *Z. Anorg. Allg. Chem.* **2002**, *628*, 133.

Table 3. Experimental and Calculated MF_6 Vibrational Frequencies (cm^{-1}) at the B3LYP/aT-PP and BP86/aT-PP Levels[a]

		a_{1g}		e_g		t_{1u}		t_{1u}		t_{2g}		t_{2u}	
MF_6	state/sym	calc	expt	calc	expt	calc	expt	calc	expt	calc	expt	calc	expt
WF_6[b]	$^1A_{1g}/O_h$	757	771[c]	665	677[c]	699(810)	711[d]	239(102)	258[d]	304	320[c]	123(0)	[127][c]
ReF_6[e]	$^2B_{2g}/D_{4h}$	716	754[f]	a_{1g} 645 b_{1g} 640	[671][d]	a_{2u} 705(205) e_u 674(402)	715[d]	e_u 261(28) a_{2u} 217(29)	257[d]	e_g 467 b_{2g} 214	[295][d]	e_u 168(4) b_{2u} 118(0)	[147][f]
ReF_6[b]	$^2A_{1g}/D_{3d}$	747		420		a_{2u} 698(238) e_u 712(488)		e_u 269(40) a_{2u} 254(24)		a_{1g} 277 e_g 216		e_u 151(12) a_{1u} 133(0)	
OsF_6[e]	$^3A_{1g}/D_{4h}$	694	731[c]	b_{1g} 643 a_{1g} 629	[668][d]	e_u 693(334) a_{2u} 666(170)	720[g]	a_{2u} 282(7) e_u 245(34)	268[g]	e_g 285 b_{2g} 308	[276][d]	b_{2u} 207(0) e_u 161(4)	[205][d]
OsF_6[b]	$^3A_{1g}/D_{3d}$	729		474		a_{2u} 717(210) e_u 708(516)		e_u 279(30) a_{2u} 264(19)		a_{1g} 280 e_g 191		a_{1u} 213(0) e_u 154(8)	
IrF_6[b]	$^4A_{1g}/O_h$	704	702[c]	646	645[c]	710 (528)	719[d]	274(45)	276[d]	258	267[c]	200(0)	[206][d]
PtF_6[b]	$^3A_{1g}/D_{4h}$	664	656[c]	a_{1g} 622 b_{1g} 635	[601][g]	a_{2u} 709(135) e_u 688(202)	705[g]	e_u 290(14) a_{2u} 249(19)	273[g]	e_g 221 b_{2g} 195	[242][g]	e_u 223(8) b_{2u} 182(0)	[211][g]
PtF_6[h]	$^3A_{1g}/D_{3d}$	691		641		e_u 729(184) a_{2u} 726(91)		e_u 255(20) a_{2u} 245(10)		e_g 226 a_{1g} 223		a_{1u} 206(0) e_u 188(0)	
AuF_6[b]	$^2B_{2g}/D_{4h}$	619		b_{1g} 596 a_{1g} 589		e_u 668(40) a_{2u} 660(95)		a_{2u} 290(0) e_u 259(24)		b_{2g} 266 e_g 200		b_{2u} 234(0) e_u197(14)	
AuF_6[b]	$^2A_{1g}/D_{3d}$	611		482		a_{2u} 664(56) e_u 663(104)		e_u 278(12) a_{2u} 256(11)		a_{1g} 220 e_g 218		a_{1u} 242(0) e_u 190(6)	

[a] If active, the IR intensities (km/mol) are given in the parentheses. [b] B3LYP/aT-PP. [c] Reference 16. [d] Reference 15. [e] BP86/aT-PP level. [f] Reference 17. [g] Reference 13. [h] ADF Zora SO BLYP/TZ2P.

0.05 Å. The calculated average value for r(Pt−F) in the D_{4h} structure for PtF_6^- as well as the bond distance in the D_{3d} structure are in good agreement with the experimental value of 1.887(6) Å from the powder diffraction study.[25] We would expect the bond distance for AuF_6 to be within 0.01 Å of the experimental r_g value when it becomes available. Wessendrup[42] predicted that PtF_6^- at the B3LYP level using the small core Stuttgart pseudopotential and basis set for Pt, and aug-cc-pVDZ for F distorts to D_{4h} with axial Pt−F bonds of 1.960 Å and equatorial bonds of 1.908 Å consistent with our B3LYP optimized structures. At the CCSD(T)/CBS level, the D_{4h} structure is predicted to be more stable by 1.08 kcal/mol for AuF_6 and 1.04 kcal/mol for PtF_6^-. The O_h structure is again only less than 1 kcal/mol higher in energy. At the ZORA-SO level, both PtF_6^- and AuF_6 have O_h symmetry. Inclusion of all of the corrections leads to the D_{4h} structure being below the D_{3d} structure by 1.6 kcal/mol for PtF_6^- and by 0.9 kcal/mol for AuF_6.

AuF_6^-. AuF_6^- has O_h symmetry with a calculated Au−F distance of 1.899 Å at the CCSD(T)/aT-PP level in excellent agreement with the crystal structure values of 1.890(4) Å,[81] 1.899(3) Å,[20] and 1.881 Å[82] for the Au−F distance in the $O_2^+AuF_6^-$ crystal and of 1.91 ± 0.03 Å[82] for the Au−F distance in the [KrF][AuF_6] crystal. The X-ray structure[83] of the AuF_6^- anion in $Xe_2F_{11}^+AuF_6^-$ shows an octahedral anion with an average Au−F distance of 1.861 Å. On the basis of all of our results, this bond distance is too short as is the value of 1.874(6) Å from the powder diffraction study.[25]

Vibrational Frequencies. The six normal modes for MF_6 with O_h symmetry are ν_1 (a_{1g}), ν_2(e_g), ν_3(t_{1u}), ν_4(t_{1u}), ν_5(t_{2g}), and ν_6(t_{2u}). Under the Jahn−Teller distortion from O_h to D_{4h} the vibrational modes split as follows: $a_{1g} \rightarrow a_{1g}$, $e_g \rightarrow a_{1g} + b_{1g}$, each of the two $t_{1u} \rightarrow a_{2u} + e_u$, $t_{2g} \rightarrow b_{2g} + e_g$, and $t_{2u} \rightarrow b_{2u} + e_u$. The experimental[12−17] frequencies are compared to the B3LYP/aT-PP and/or BP86/aT-PP calculated MF_6 vibrational frequencies and their infrared intensities in Table 3 for M = W, Ir, Pt, and Au. For M = Re and Os, the B3LYP calculations gave two artificial imaginary frequencies possibly because of symmetry breaking, so we used the BP86/aT-PP frequencies. WF_6 and IrF_6, which have zero and three d electrons, respectively, have O_h symmetry and do not exhibit splitting of the vibrational modes. Our calculated values at the B3LYP/aT-PP level are smaller than the experimental values by 4 to 19 cm^{-1} for WF_6, and larger by 1 to 9 cm^{-1} for IrF_6, showing excellent agreement between theory and experiment. Weinstock et al.[13] interpreted the spectra of ReF_6, OsF_6, and PtF_6 assuming O_h symmetry, but noted that the vibrational mode ν_2 of symmetry e_g appears to be less intense for ReF_6 and OsF_6 and has a broader shape than for the other studied hexafluorides (SF_6, SeF_6, MoF_6, TeF_6, WF_6, UF_6, PtF_6, NpF_6, and PuF_6). This was considered to be evidence for a Jahn−Teller effect. Our calculated ReF_6 frequencies can qualitatively be compared to the experimental values. The a_{1g} stretch is smaller than the experimental one by 38 cm^{-1}, and the e_g and t_{1u} stretches split by 31 cm^{-1} with their averages being in reasonable agreement with experiment. The lower t_{1u} mode splits by about 44 cm^{-1} and the t_{2u} mode by 50 cm^{-1}, and both averages are qualitatively in agreement with experiment. The t_{2g} scissoring mode shows a large splitting of 253 cm^{-1}, and the average is in poor agreement with experiment. Similar values have been obtained for OsF_6 with the stretches showing small splittings with averages in agreement with experiment. The calculated frequencies for PtF_6 are in good agreement with experiment with only small splittings, even for the t_{2g} mode. For AuF_6, our calculated values follow the same trends as for the other compounds with only a small splitting for the t_{2g} mode.

In many of these MF_6 compounds, the t_{2g} scissoring mode shows a very unusual behavior. It exhibits large splittings and, above all, the frequency order of the split components in ReF_6 and PtF_6 is reversed from that in

(81) Graudejus, O.; Muller, B. G. *Z. Anorg. Allg. Chem.* **1996**, *622*, 1076.
(82) Lehmnann, J. F.; Schrobilgen, G. J. *J. Fluorine Chem.* **2003**, *119*, 109.
(83) Leary, K.; Zalkin, A.; Bartlett, N. *Inorg. Chem.* **1974**, *13*, 775.

OsF_6 and AuF_6. An inspection of the appropriate symmetry coordinates involved (Figure 2) provides a ready explanation. On lowering the symmetry from O_h to D_{4h}, the four equatorial and the two axial M−F bonds no longer possess the same bond lengths and the O_h t_{2g} mode splits into a b_{2g} equatorial scissoring mode and an e_g axial scissoring mode. If the equatorial M−F bonds are the shorter and stronger ones, the equatorial b_{2g} scissoring mode should have the higher frequency, and when the axial M−F bonds are shorter, the e_g axial scissoring mode should have the higher frequency. This is exactly the case. In ReF_6 and PtF_6 with shorter axial bonds, the e_g axial deformation modes have the higher frequencies, while in OsF_6 and AuF_6 with longer axial bonds the b_{2g} equatorial scissoring modes have the higher frequencies.

The frequencies for the D_{3d} structures are similar to those of the D_{4h} structures. The biggest differences are found for ReF_6 and OsF_6 for the modes derived from the e_g stretching mode in the O_h structures. This mode is not split in D_{3d} symmetry as it is in D_{4h} symmetry and is ∼200 and 150 cm^{-1} lower than the average of the a_{1g} and b_{1g} modes in D_{4h} symmetry for ReF_6 and OsF_6, respectively.

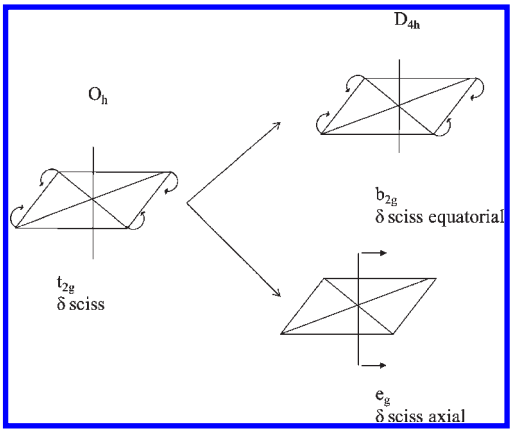

Figure 2. Symmetry coordinates for the MF_6 scissoring mode splitting into its two components, i.e., equatorial and axial scissoring upon lowering of the symmetry from O_h to D_{4h}. When the four equatorial bonds are shorter than the axial ones, the b_{2g} mode has the higher frequency and, when they are longer, the axial e_g deformation has the higher frequency.

Of interest to the prediction of the thermodynamic properties are the differences between the calculated and experimental zero point energies (ZPEs). These are compared in Table 6. All ZPEs calculated at the B3LYP level are within 0.3 kcal/mol of the experimental values as is the ZPE calculated at the BP86 level for ReF_6. The ZPE calculated at the BP86 level for OsF_6 is about 0.4 kcal/mol too small and is about 0.5 kcal/mol too small for WF_6.

Electron Affinities and Oxidizer Strengths. Table 4 lists the valence CBS energies, the various additive energy corrections, and the calculated composite electron affinities, which are compared with the experimental values. The ZPE correction, calculated at the BP86/aD-PP or B3LYP/aT-PP levels, slightly increases the electron affinities (except for the EAs of WF_6 and PtF_6), whereas the core−valence correction, calculated at the CCSD(T)/awCVTZ level slightly decreases the electron affinities except for WF_6. An energy diagram showing the different states for the anions and neutrals used in predicting the electron affinities is shown in Figure 1.

If spin orbit interactions are not included, the electron affinity does not increase across the row, which is inconsistent with the prediction by Bartlett[6] that EA(IrF_6) is less than EA(OsF_6). Without spin orbit, the electron affinities of the MF_6 compounds follow the behavior expected for filling the t_{2g} orbitals (d_{xy}, d_{xz}, d_{yz}) as we increase the atomic number from W to Au. The electron affinity increases from WF_6 to OsF_6 as electrons are added to the t_{2g} orbitals. The most stable species in this sequence is OsF_6^- which has 3 unpaired d electrons satisfying Hund's rule and would be expected to have the highest ionization potential like N in the first row (resulting in the highest electron affinity for OsF_6). Additional d electrons force spin pairing to occur and, as in the first row, the ionization potential of the anion (electron affinity of the corresponding neutral) would be expected to drop just as in main group elements. The ionization potential increases for AuF_6^- because it has a completely filled shell just like a noble gas. The filling of the d orbitals

Table 4. Energy Components for the Calculated Electron Affinities (in kcal/mol)

	state/sym								
M	MF_6	MF_6^-	ΔE_{CBS}[a]	ΔE_{ZPE}	ΔE_{CV}[b]	ΔE_{rel}[c]	EA	SO[d]	EA +SO
W	$^1A_{1g}/O_h$	$^2B_{2g}/D_{4h}$	67.36	0.73[e]	0.45	2.36	70.9	1.90	72.8
	$^1A_{1g}/O_h$	$^2A_{1g}/D_{3d}$	67.34	1.00[e]	0.34	2.35	71.0	1.31	72.3
Re	$^2A_{1g}/D_{3d}$	$^3A_{1g}/D_{4h}$	103.45	−0.01[f]	−0.17	1.38	104.7	0.88	105.6
	$^2B_{2g}/D_{4h}$	$^3A_{1g}/D_{4h}$	103.20	0.77[f]	−0.20	1.39	105.2	1.11	106.3
	$^2A_{1g}/D_{3d}$	$^3A_{1g}/D_{3d}$	102.41	0.90[f]	−0.14	1.18	104.4	1.00	105.4
Os	$^3A_{1g}/D_{4h}$	$^4A_{1g}/O_h$	138.30	0.91[f]	−0.71	0.29	138.8	−2.30	136.5
	$^3A_{1g}/D_{3d}$	$^4A_{1g}/O_h$	139.14	0.55[f]	−0.76	0.28	139.2	−2.45	136.7
Ir	$^4A_{1g}/O_h$	$^3A_{1g}/D_{4h}$	130.85	0.72[f]	−1.01	1.59	132.2	5.98	138.2
	$^4A_{1g}/O_h$	$^3A_{1g}/D_{3d}$	130.08	1.43[f]	−0.94	1.61	132.2	5.98	138.2
Pt	$^3A_{1g}/D_{4h}$	$^2B_{2g}/D_{4h}$	163.10	0.57[e]	−1.43	0.74	163.0	0.62	163.6
	$^3A_{1g}/D_{3d}$	$^2A_{1g}/D_{3d}$	162.49	0.76[e]	−1.32	0.98	162.9	0.61	163.5
Au	$^2B_{2g}/D_{4h}$	$^1A_{1g}/O_h$	194.25	0.30[g]	−1.42	−0.05	193.1	−3.90	189.2
	$^2A_{1g}/D_{3d}$	$^1A_{1g}/O_h$	195.34	−0.06[g]	−1.54	−0.06	193.7	−3.63	190.1

[a] Valence CCSD(T) electronic energy contribution extrapolated using the mixed Gaussian/exponential formula. [b] Core−valence correction obtained at the CCSD(T)/awCVTZ level. [c] See eq 1. [d] Spin−orbit correction from BLYP/ZORA + SO/TZ2P calculation. [e] ADF Zora SO BLYP/TZ2P. [f] BP86/aD-PP. [g] B3LYP/aT-PP.

Table 5. Adiabatic Electron Affinities of MF_6, Vertical Electron Detachment Energies (VDE) of MF_6^-, and Vertical Electron Attachment Energies (VAE) of MF_6 (in kcal/mol) Calculated at the CCSD(T)/aT-DK//CCSD(T)/aT-PP Level

molecule	MF_6 state/sym	MF_6^- state/sym	ADE	VDE[a]	VAE[b]
WF_6/WF_6^-	$^1A_{1g}/O_h$	$^2B_{2g}/D_{4h}$	68.7	79.4	54.1
ReF_6/ReF_6^-	$^2A_{1g}/D_{3d}$	$^3A_{1g}/D_{4h}$	103.8	115.0	94.7
ReF_6/ReF_6^-	$^2B_{2g}/D_{4h}$	$^3A_{1g}/D_{4h}$	103.6	115.0	88.4
OsF_6/OsF_6^-	$^3A_{1g}/D_{4h}$	$^4A_{1g}/O_h$	137.8	144.7	128.5
IrF_6/IrF_6^-	$^4A_{1g}/O_h$	$^3A_{1g}/D_{4h}$	130.5	136.1	123.3
PtF_6/PtF_6^-	$^3A_{1g}/D_{4h}$	$^2B_{2g}/D_{4h}$	161.7	166.7	154.6
AuF_6/AuF_6^-	$^2B_{2g}/D_{4h}$	$^1A_{1g}/O_h$	191.8	196.4	191.7

[a] VDE = $E_{\text{neutral at anion geom}} - E_{\text{anion}}$. [b] VAE = $E_{\text{neutral}} - E_{\text{anion at neutral geom}}$.

in the transition metal hexafluorides differs from that of the s/p orbitals in main group fluorides. In the transition metal hexafluorides, the formal oxidation state of the central atom remains constant at +6 and does not change, contrary to the main group fluorides.

The SO correction (Table 4) to the EA was calculated as the difference between EA(ZORA+SO) and EA(ZORA). The electron affinities calculated with ZORA and ZORA+SO are given in the Supporting Information. The effect of the SO correction is to increase the electron affinities for WF_6, ReF_6, IrF_6, and PtF_6 and to decrease those for OsF_6 and AuF_6. The SO effect on the electron affinity of OsF_6 is to decrease the EA by 2.67 kcal/mol and, for IrF_6, to increase it by 5.98 kcal/mol. When added to the CCSD(T) values, these SO corrections have the effect of reversing the order of the electron affinities for OsF_6 and IrF_6 so that EA(IrF_6) is greater than EA(OsF_6) by 0.07 eV. Thus, inclusion of molecular spin−orbit corrections results in a monotonic increase of the EAs for the third row transition metal hexafluorides. *The inclusion of molecular spin−orbit effects is essential for predicting the correct ordering of the electron affinities for these metal hexafluorides.*

Our calculated value of 3.15 eV for WF_6, which includes all corrections, differs from the ICR bracketing experimental[8] value of 3.5 eV. This difference of 0.35 eV is larger than expected on the basis of the agreement with experiment to within about 0.1 eV for the electron affinities of the metal oxide compounds[84] (WO_3 and W_2O_6), where W is also in the +6 oxidation state. Our calculated value is, however, in good agreement with the lower error bar of the $3.36^{+0.4}_{-0.2}$ eV value reported by Viggiano et al.[9] In the first bracketing study,[8] EA(WF_6) was estimated to be 3.5 eV between EA(F)[85] = 3.401 eV and EA(Cl) = 3.612 eV on the basis of the observation that WF_6 reacts with F^- in both charge transfer and association reactions but not with Cl^-. Viggiano et al.[9] did not observe charge transfer in the reaction of WF_6 with F^- and only observed the association reaction. They did observe charge transfer from Br^- to WF_6 so EA(WF_6) > EA(Br) = 3.364 eV. The lower error bar limit of 0.2 eV was estimated from the internal energy of WF_6 and translational energy effects. Thus, our calculated EA(WF_6) value is consistent with the lower end of the energy range of Viggiano et al.[9]

The calculated electron affinities for OsF_6 and PtF_6 are in very good agreement with those from the charge transfer experiments by Sidorov and co-workers et al.[10] The calculated value of the electron affinity for IrF_6 is lower and lies just outside the experimental charge transfer error bar.[10] Friedman et al.[86] used a flowing afterglow to show that EA(ReF_6) > EA(MoF_6) = 3.8 ± 0.2 eV and our calculated value is consistent with this experimental result.[87] On the basis of experiments such as the oxidation of NO and ONF by MF_6, Bartlett developed a scale of electron affinities. Our results are in good agreement with his approximate values and with the result that EA(IrF_6) > EA(OsF_6).

Lower level calculations of the EAs as summarized in Table 1 are generally in agreement with our CCSD(T) values. We note that the CI-SD+Q values for WF_6[39] and AuF_6[40] are too large as compared to our values and those of others. The CCSD(T)/DZP calculation[42] for PtF_6 is in good agreement with our larger basis set value. The early DV-Xα values[37] are in reasonable agreement with our values except for IrF_6 which is 1 eV too large; these values are not purely theoretical as they are set relative to an experimental value of 3.5 eV for WF_6. The DFT/TZP/BP values[41] are in good agreement with our values for WF_6 and ReF_6 but start to show larger deviations beginning with OsF_6.

Vertical electron detachment (VDE) and attachment (VAE) energies have been calculated for the third row transition metal hexafluorides at the different levels of theory with the aT-PP basis set (Table 5) as these values are relevant to experimental measurements. The VDE of MF_6^- was calculated from the difference between the energy of the neutral species MF_6 calculated at the corresponding anion geometry and the energy of the MF_6^- species. For the VAEs of MF_6, we calculated the energies of the anions at the geometries of the neutrals and subtracted them from the MF_6 energies. The VDEs of MF_6^- are 3 to 10 kcal/mol larger than the adiabatic EAs, and the VAEs are 2 to 20 kcal/mol smaller than the adiabatic EAs. The largest differences between the VDEs and VAEs and the adiabatic EAs occur for the earlier transition metal atoms, and the differences from the adiabatic EAs become much smaller as one proceeds from W to Au. For Au, the adiabatic EA, VDE, and VAE are all quite similar.

At the CCSD(T) level, we found a difference of less than 4 kcal/mol between the calculated values of the EAs with the aD-PP and aT-PP basis sets and of ≤1.5 kcal/mol between the aT-PP and aQ-PP basis sets (see Supporting Information). At the Hartree−Fock (HF) level a larger dependence was found, as the aD-PP and aT-PP values differ by an average of 6 kcal/mol with larger differences for the early metals of the series. The HF EAs are larger than the correlated EAs, and as one improves the correlation treatment, the EA decreases. This is opposite to what happens in typical electron affinities where the inclusion of the correlation energy in most cases leads to an increase in the electron affinity if the neutral molecule and its

(84) Li, S.; Dixon, D. A. *J. Phys. Chem. A* **2007**, *111*, 11908.
(85) Blondel, C.; Delsart, C.; Goldfarb, F. *J. Phys. B.* **2001**, *34*, L281.
(86) Friedman, J. F.; Stevens, A. E.; Miller, T. M.; Viggiano, A. A. *J. Chem. Phys.* **2006**, *124*, 224306.
(87) Miller, T. M. In *Handbook of Chemistry and Physics*, 86th ed.; Lide, D. R., Ed.; CRC: Boca Raton, FL, 2005; Sec. 10, pp 156−172.

Table 6. Calculated Energy Components for Total Atomization Energies (TAE = $\sum D_0$) for MF_6 (in kcal/mol) at 0 K

molecule	state/sym	ΔE_{CBS}[a]	ΔE_{ZPE}	ΔE_{CV}[b]	ΔE_{rel}[c]	atomic ΔE_{SO}[d]	$\sum D_{0,0K}$[e]
WF_6	$^1A_{1g}/O_h$	759.29	−8.83[f](−9.10)[g]	−0.20	−4.22	−2.33	735.27
ReF_6	$^2A_{1g}/D_{3d}$	629.69	−8.07[f]	0.78	−2.56	−2.33	617.51
ReF_6	$^2B_{2g}/D_{4h}$	629.94	−9.14[h](−9.05)[g]	0.82	−2.58	−2.33	616.71
OsF_6		566.19	−8.86[h](−9.25)[g]	1.59	−1.83	−9.90	547.19
IrF_6	$^4A_{1g}/O_h$	495.99	−9.03[f](−9.14)[g]	2.66	−2.16	−12.71	474.75
PtF_6		381.37	−8.72[f](−8.79)[g]	11.70	1.12	−2.33	371.60
AuF_6	$^2B_{2g}/D_{4h}$	252.57	−8.44[f]	9.84	1.20	−2.33	252.84

[a] $\Delta E = \Delta E(M) + 6\Delta E(F) - \Delta E(MF_6)$. [b] CCSD(T)/awCVTZ. [c] See eq 1. [d] The spin−orbit splitting is −0.39 kcal/mol for the ($^2P_{3/2}$) state of F. See text for the metals. [e] $\sum D_{0,0K} = \Delta E_{CBS} + \Delta E_{ZPE} + \Delta E_{CV} + \Delta E_{rel} + \Delta E_{SO}$. [f] B3LYP/aT-PP. [g] Experimental ZPE's. [h] BP86/aT-PP.

Table 7. Calculated and Experimental Values for $\Delta H_{f,0K}$ and $\Delta H_{f,298K}$ for MF_6 (in kcal/mol)[a]

molecule	MF_6 state/sym	$\Delta H_{f,0K}$[b]	$\Delta H_{f,298K}$[b]	$\Delta H_{f,0K}$[c]	$\Delta H_{f,298K}$[c]	exp
WF_6	$^1A_{1g}/O_h$	−421.4	−423.0			−422.0 ± 4,[29] −411.5 ± 0.4,[30] −411.7 ± 0.5,[31] −411.4 ± 0.2[32]
ReF_6	$^2B_{2g}/D_{4h}$	−322.1	−323.0	−319.7	−321.6	−322.6 ± 2.3[33]
ReF_6	$^2A_{1g}/D_{3d}$	−322.9	−323.3	−320.5	−321.9	
OsF_6	$^3A_{1g}/D_{4h}$	−247.6	−248.4	−247.3	−249.1	
IrF_6	$^4A_{1g}/O_h$	−205.1	−206.0	−204.0	−205.9	−130.0[34]
PtF_6	$^3A_{1g}/D_{4h}$	−125.9	−126.6	−130.6	−132.3	−161.6 ± 6.7,[34] −160.6 ± 1.5[35]
AuF_6	$^2B_{2g}/D_{4h}$	−54.5	−55.0	−51.4	−53.1	

[a] Heat of formation of F for all from the JANAF Tables. $\Delta H_{f,298K}(MF_6) = \Delta H_{f,0K}(MF_6) + \Delta H_{0K\rightarrow 298K}(MF_6) - \Delta H_{0K\rightarrow 298K}(M) - 6\Delta H_{0K\rightarrow 298K}(F)$. The experimental enthalpy change from 0 to 298 K ($\Delta H_{0K\rightarrow 298K}$) is 1.05 for F and 1.19 kcal/mol for W. For Re, Os, Ir, Pt, and Au we have used a value of 1.20 kcal/mol. [b] Wagman et al. values[75] for all metals except for W from JANAF Tables.[28] [c] Greenwood and Earnshaw[76] values for all metals.

anion can be treated reasonably well with a single configuration wave function. In most of the simple molecules in which this is observed, the electron is added to a diffuse orbital that is on the exterior of the molecule. In these transition metal hexafluorides, however, the electron is added to a metal d orbital of the M(+6) center and is surrounded by negatively charged ligands (F^-). This difference between the HF and correlated values has been observed previously for WF_6 and attributed to the reduction of intraclosed shell correlation in the anions.[39]

One of the most fascinating problems from the onset of third row transition metal hexafluoride chemistry was concerned with the relative oxidizer strengths of these highly unusual oxidizers, and experiments were undertaken to establish qualitative measures for their oxidizing power based on their reaction chemistry.[7] In the following simple Born−Haber cycle for the one-electron oxidation of a given substrate S,

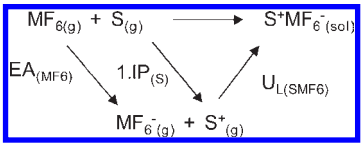

the free energy change of the reaction is a measure of the oxidizing power of MF_6. The free energy is given by the sum of the electron affinity of MF_6, the first ionization potential of S (1.IP), and the lattice energy of $S^+MF_6^-$. Since for a given substrate, 1.IP is always the same and the lattice energies of SMF_6 do not change much because of the radii of the MF_6^- being almost identical, the oxidizer strength of MF_6 is governed almost exclusively by the electron affinity of MF_6. Therefore, the oxidizer strength increases monotonically from WF_6 to AuF_6 with PtF_6 being the strongest presently known oxidizer within this series, and the electron affinity of MF_6 (Table 1) being an excellent quantitative measure of its oxidizing power.

Heats of Formation. The total atomization energies (TAEs) (Table 6) which yield $\Delta H_{f,0K}$ and $\Delta H_{f,298K}$ (Table 7) were calculated at the CCSD(T) level, and an atomic spin orbit correction is required.[74] The spin−orbit splitting is 0.39 kcal/mol for the ($^2P_{3/2}$) state of F. The ground states of Re ($^6S_{5/2}$) and Au ($^2S_{1/2}$) do not have any spin orbit splitting, so they can be used directly to calculate the TAEs. For M = W, we calculated the TAE relative to the $^7S_3$ excited state of the atom which has no spin orbit correction and corrected the calculated TAE with the experimental energy difference of 8.44 kcal/mol with respect to the $^5D_0$ ground state. For Pt, we used a similar approach and calculated the TAE for the $^1S_0$ excited state which was corrected by an energy difference of 17.54 kcal/mol with respect to the $^3D_3$ ground state. For Os and Ir, there are no convenient low lying excited states so we used the experimental ground states of Os ($^5D_4$) and Ir ($^4F_{9/2}$) with J-averaged spin orbit corrections of −7.57 and −10.38 kcal/mol, respectively. The TAEs decrease in the series from WF_6 to AuF_6.

We compare our calculated heats of formation with the available experimental values (Table 7). Excellent agreement is found between our calculated results and the experimental values for $\Delta H_f(WF_6)$, −423.2 versus −422.0 kcal/mol,[30] and for $\Delta H_f(ReF_6)$, −321.8 versus −322.6 kcal/mol.[33] Other experimental values reported for $\Delta H_f(WF_6)$ are −411.5 ± 0.4,[30] −411.7 ± 0.5,[31] and −411.5 ± 0.2,[32] which are too positive. For PtF_6 the difference between our calculated value and the experimental estimate is 29 kcal/mol. Clearly, the prediction of $\Delta H_{f,298K}(IrF_6)$ = −130.0 kcal/mol, made by Ruff in 1929,[34] is incorrect.

What are the sources of errors in the calculated heats of formation of these metal fluorides? The first one is the experimental heat of formation of the metal atom, as the heats of formation of these transition metal atoms in the gas phase are not as well established and have larger error bars than do most main group elements

Table 8. Calculated Energy Components for the First Adiabatic and Average M−F Bond Dissociation Energies of MF_6 (in kcal/mol)

	state/sym								
M−F Bond	MF_5[a]	MF_6	ΔE_{CBS}[b]	ΔE_{ZPE}[c]	ΔE_{CV}[d]	ΔE_{rel}[e]	ΔE_{SO}[f]	1st BDE[g]	Avg BDE[h]
W−F	$^2A_2/C_{2v}$	$^1A_{1g}/O_h$	124.0	−2.31[i]	0.13	−2.64	−1.51	117.7	122.5
Re−F	$^3A_1'/D_{3h}$	$^2B_{2g}/D_{4h}$	90.6	−2.54[j]	1.19	−1.63	1.10	88.7	102.8
Re−F	$^3A_1'/D_{3h}$	$^2A_{1g}/D_{3d}$	90.4	−1.30[k]	1.15	−1.86	1.33	89.7	102.9
Os−F	$^4B_1/C_{4v}$	$^3A_{1g}/D_{4h}$	74.0	−2.55[k]	1.72	−0.96	2.02	74.2	91.2
Ir−F	$^5B_1/C_{4v}$	$^4A_{1g}/O_h$	85.9	−2.31[i]	1.15	−0.69	−9.78	74.3	79.1
Pt−F	$^2B_1/C_{4v}$	$^3A_{1g}/D_{4h}$	45.1	−1.97[i]	2.52	−1.17	1.87	46.4	61.9
Au−F	$^1A_1/C_{4v}$	$^2B_{2g}/D_{4h}$	25.0	−2.24[i]	2.33	0.20	0.25	25.5	42.1

[a] All MF_5 structures optimized at the DFT level with the B3LYP functional with the aT-PP basis sets. DFT optimized geometries plus the scalar relativistic ZORA and ZORA-SO optimized geometries at the BLYP/TZ2P level are in Supporting Information [b] Single point energies extrapolated to the CBS limit calculated at the CCSD(T) level with aD-PP, aT-PP and aQ-PP basis sets using the B3LYP/aT-PP geometries. [c] ZPE at the B3LYP or BP86 levels, [d] Core−valence corrections at the CCSD(T)/awCVTZ level. [e] See eq 1. [f] SO correction at the ADF ZORA BLYP/TZ2P level plus the experimental spin−orbit correction of −0.39 kcal/mol for F. [g] 1st BDE calculated as the sum of ΔE_{CBS} and of all corrections. [h] Average BDE = $\sum D_{0,0K}$ (MF_6)/6. [i] BP86/aD-PP. [j] BP86/aT-PP. [k] B3LYP/aT-PP.

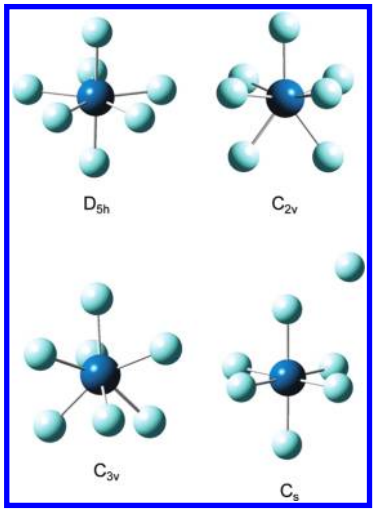

Figure 3. Optimized geometries for the four different structures for MF_7^- as exemplified by WF_7^- or PtF_7^-. The structures are pentagonal bipyramid (D_{5h}), monocapped octahedron (C_{3v}), monocapped trigonal prism (C_{2v}), and the non-classical (C_s).

(see Supporting Information). The error bars reported by Greenwood and Earnshaw[76] are not small and can be as large as ± 5.0 kcal/mol. The NBS tables[75] do not provide error bars, and although there is good agreement for $\Delta H_{f,298K}$ for W, Os, and Ir between references 75 and 76, there is not as good an agreement for the other metals. Thus, it is likely that the largest source of error in the predicted heats of formation is due to the metal atomic values. The accurately calculated TAEs could be used together with experimental heats of formation of the fluorides, determined without the use of atomic energies, to obtain the heats of the atoms as has been done for ΔH_f(B).[88] An additional source of error in the calculated heats of formation is due to the spin orbit correction for the metal atoms, as it is not clear whether the J-averaged approach for the atomic spin orbit correction that we have taken from our work on main group elements[77] can be applied as reliably to the transition metals with more low lying excited states. As discussed above, the errors in the ZPEs are on the order of at most 0.5 kcal/mol. The last source of error is the molecular spin orbit effect, which was not included in the calculated heats of formation because of the difficulty in calculating the appropriate quantity for the atoms.

Bond Dissociation Energies. Average adiabatic bond dissociation energies (BDEs) are calculated from the total atomization energies and are given in Table 8. The BDEs decrease in the series from WF_6 to AuF_6 consistent with the increase in bond length. Our findings are consistent with Bartlett's[7] prediction that the more powerful oxidizers in the MF_6 series (higher electron affinity) have lower average bond energies than the weaker oxidizers (lower electron affinity). Our calculated average M−F BDEs are quite high for the early metals of the series. The average BDEs range from 122.5 kcal/mol for the W−F bond energy to 42.1 kcal/mol for Au−F. The W−F BDE is only ~7 kcal/mol less than the C−F BDE in CF_4 and ~43 kcal/mol less than the Si−F BDE in SiF_4.[89]

The first adiabatic M−F BDEs have been calculated at different levels of theory from the reaction $MF_6 \rightarrow MF_5 + F$ with all species in their ground states (Table 8). DFT optimized geometries at the B3LYP/aT-PP level as well as scalar relativistic ZORA and ZORA-SO optimized geometries at the BLYP/TZ2P level are given in Supporting Information. Different molecular geometries and spin states were examined considering the way d orbitals split in the trigonal bipyramidal (D_{3h}) and square pyramidal (C_{4v}) ligand fields. WF_5 with only one 5d electron distorts from the square pyramidal C_{4v} structure to a C_{2v} ($^2A_2$) structure with an average bond length of 1.854 Å. ReF_5 with two 5d electrons has a $^3A_1'/D_{3h}$ ground state with an average bond length of 1.851 Å; the $^3A_1'/D_{3h}$ state is ~6 kcal/mol more stable than the C_{4v} structure. OsF_5 with three 5d electrons has a $^4B_1/C_{4v}$ ground state with an average bond distance of 1.858 Å. Of all possible states for IrF_5, the $^5B_1/C_{4v}$ state is the most stable with an average bond distance of 1.875 Å. The $^1A_1$ and $^3A_1$ C_{4v} symmetry structures for IrF_5 are 9.9 and 4.7 kcal/mol higher in energy, respectively. The D_{3h} states for IrF_5 are up to 20 kcal/mol higher in energy than the $^5B_1/C_{4v}$ ground state. The PtF_5 $^2B_1/C_{4v}$ ground state has an average bond distance of 1.870 Å. The $^1A_1/C_{4v}$ ground state of AuF_5 has an average bond distance of 1.894 Å. The average M−F bond distances in the MF_5 series are

(88) Karton, A.; Martin, J. M. L. *J. Phys. Chem. A* **2007**, *111*, 5936.

(89) Luo, T.-R. *Comprehensive Handbook of Chemical Bond Energies*; CRC Press, Taylor & Francis Group: Boca Raton, FL, 2007.

Table 9. Calculated MF_6 Fluoride Affinities and MF_6^-−F Bond Dissociation Energies (in kcal/mol)

	state/sym										
M	MF_6	$MF_7^{-a,b}$	CCSD(T)/aD	CCSD(T)/aT	ΔE_{CBS}[c]	ΔE_{ZPE}	ΔE_{CV}[d]	ΔE_{rel}[e]	ΔE_{SO}[f]	FA	BDE[g]
W	$^1A_{1g}/O_h$	$^1A_1'/D_{5h}$	76.63	77.91	78.08	−0.97[h]	0.04	0.96	0.01	78.1	83.7
W	$^1A_{1g}/O_h$	$^3A''/C_s$	−3.16	−9.02		1.19[i]				−7.8	3.5[j]
Re	$^2B_{2g}/D_{4h}$	$^2A_2/C_{2v}$	79.86	80.97	81.00	0.02[k]	0.33	0.18	−0.67	80.9	53.0
Re	$^2B_{2g}/D_{4h}$	$^4A''/C_s$	33.46	27.12		−0.40[i]				26.7	2.1[j]
Re	$^2A_{1g}/D_{3d}$	$^2A_2/C_{2v}$	80.08	81.21	81.25	−0.9[l]	0.36	0.41	−0.90	80.2	53.0
Re	$^2A_{1g}/D_{3d}$	$^4A''/C_s$	33.68	27.36		0.07[l]				27.4	3.4
Os	$^3A_{1g}/D_{4h}$	$^3A_1'/D_{5h}$	86.02	86.83	86.34	−0.90[k]	0.40	0.48	−3.85	82.5	24.4
Os	$^3A_{1g}/D_{4h}$	$^5A''/C_s$	68.30	61.46		1.23[i]				62.7	2.7[j]
Ir	$^4A_{1g}/O_h$	$^2B_1/C_{2v}$	61.80	62.72	64.18	−0.28[m]	2.21	1.42	2.49	70.0	10.2
Ir	$^4A_{1g}/O_h$	$^2A'/C_s$	34.01	30.42		1.06[i]				31.5	−19.8[j]
Pt	$^3A_{1g}/D_{4h}$	$^1A_1'/D_{5h}$	83.43	84.32	84.17	−1.08[m]	−0.61	0.13	−3.65	79.0	−6.2
Pt	$^3A_{1g}/D_{4h}$	$^3A'/C_s$	90.51	85.75		−0.16[i]		−1.30	0.08	84.4	−0.1[n]
Au	$^2B_{2g}/D_{4h}$	$^2B_2/C_{2v}$	87.82	83.91	83.30	−0.06[m]	−1.83	0.30	−3.24	78.5	−32.3
Au	$^2B_{2g}/D_{4h}$	$^2A'/C_s$	119.52	115.68		−0.23[i]		0.24	−3.93	111.8	2.0[n]

[a] See Supporting Information for details of calculations on MF_7^-. [b] The second row for each metal is for the MF_7^- non-classical structure. [c] Extrapolated using the mixed Gaussian/exponential formula. [d] CCSD(T)/awCVTZ. [e] See eq 1. [f] SO correction at the ADF ZORA BLYP/TZ2P level. [g] BDE = EA(F) − EA (MF_6) + FA (MF_6) (see text). [h] MP2/aD-PP. [i] B3LYP/aD-PP. [j] CCSD(T)/aT-PP values for the EA and FA(MF_6) are used together with the ZPE. [k] BP86/aT-PP. [l] BP86/aD-PP. [m] B3LYP/aT-PP. [n] CCSD(T)/aT-PP values for the EA and FA(MF_6) are used together with the ZPE, ΔE_{rel}, and ΔE_{SO} corrections.

approximately constant for M = W, Re, Os, increase in IrF_5 and PtF_5, and increase further in AuF_5. This trend is similar to that found for the metal hexafluorides (Table 2) where the average M−F bond distances are about the same from WF_6 through IrF_6 and then increase for PtF_6 and AuF_6.

The first adiabatic BDEs follow the same trend as the average BDEs and are up to 20 kcal/mol lower than the average BDEs, except for the first BDE for Ir−F, which is ∼5 kcal/mol higher than its average BDE. The first BDEs as a function of the basis set are given in the Supporting Information and show that the effect of the basis set is not negligible even with the aT-PP basis set. The spin orbit corrections to the first BDEs were calculated to be less than 2 kcal/mol for all species except for M = Ir. The $^1A_{1g}$ state of WF_6 should be affected less by spin orbit coupling than the $^2A_2$ state of WF_5, so the total spin orbit effect reduces its first BDE. For AuF_6, the spin orbit effect for the $^1B_{2g}$ state nearly cancels that for the $^1A_1$ state of AuF_5 plus that for the F atom. For M = Re, Os, and Pt, the spin orbit corrections to the first BDEs depend on the relative magnitude of the spin orbit effects in MF_6 and MF_5, and our calculations show they all increase the first BDEs by 1 to 2 kcal/mol. For IrF_6, the $^4A_{1g}$ state has a much smaller spin orbit correction as compared to the $^5B_1$ state of IrF_5, as the former has the degenerate t_{2g} orbitals half-filled. The total spin orbit correction substantially reduces the first BDE of IrF_6 by ∼10 kcal/mol. The calculated spin orbit contributions for the first BDEs clearly show their importance, and significant error can be introduced if they are not included.

Fluoride Affinities and Lewis Acidities. Table 9 lists the valence CBS energies and the various additive corrections included in the calculation of the MF_6 fluoride affinities. The results from DFT calculations with a selection of functionals and fluoride affinities calculated as a function of basis set at different levels of theory are given in the Supporting Information.

The anionic heptafluorides have the same number of d electrons as the neutral hexafluorides. The addition of an F^- to an octahedral MF_6 structure would be expected to lead to three possible geometries (Figure 3) on the basis of main group structures: pentagonal bipyramid (PBP, D_{5h}), monocapped octahedron (MCO, C_{3v}), and monocapped trigonal prism (MCTP, C_{2v}). Lin and Bytheway[90] predicted for WF_7^- that the MCO is more stable than the MCTP and the PBP by 0.1 and 1 kcal/mol, respectively, at the HF level; the MCTP and PBP structures had 1 and 2 imaginary frequencies. We found that at the B3LYP/aD-PP level, all three geometries have imaginary frequencies: two of $18i$ $cm^{-1}$for PBP, two of $34i$ cm^{-1} for MCO, and one of $18i$ cm^{-1} for MCTP, consistent with the other DFT calculations on similar molecules.[91] All three are very close in energy with the MCO and MCTP structures being only 0.71 and 0.57 kcal/mol higher in energy, respectively, relative to the PBP at the B3LYP/aD-PP level. At the CCSD(T)/CBS level these differences are 0.66 for the MCO structure and 0.64 kcal/mol for the MCTP structure with respect to the lowest energy PBP structure. ReF_7^- with one 5d electron distorts to a doublet C_{2v} structure (not MCTP) which is a PBP structure distorted in the plane and more stable than the MCTP structure by 3.6 kcal/mol. The OsF_7^- PBP structure is lower in energy than the MCO and the MCTP structures by 5.6 and 4.9 kcal/mol, respectively; the two higher energy structures have imaginary frequencies of $74i$ cm^{-1} and $92i$ cm^{-1} respectively. IrF_7^-, like ReF_7^-, distorts to a doublet C_{2v} structure (an in-plane distorted PBP structure), which is more stable than the MCTP structure by 24.3 kcal/mol. For PtF_7^- with four 5d electrons, the PBP structure is more stable than the MCTP by ∼4 kcal/mol, which has one imaginary frequency of $68i$ cm^{-1}.

For the three structures described above, the lowest energy structure for AuF_7^- with five 5d electrons is a doublet MCTP structure which is 37.4 kcal/mol lower in energy than a quartet PBP structure. However, the calculations at the B3LYP/aD-PP level showed two imaginary frequencies for the MCTP structure of $356i$ and $51i$ cm^{-1}, and one imaginary frequency of $277i$ cm^{-1} at the BP86/aT-PP level. The structures were distorted

(90) Lin, Z.; Bytheway, I. *Inorg. Chem.* **1996**, *35*, 594.
(91) Christe, K. O.; Curtis, E. C.; Dixon, D. A. *J. Am. Chem. Soc.* **1993**, *115*, 1520.

along the imaginary frequency direction and reoptimized. The reoptimization led to a C_s structure with one F atom bonded to an F atom ligand of the MF_6^- cluster for AuF_7^-, and we found a similar result for PtF_7^-. The new structures, $^2A'/C_s$ for AuF_7^- and $^3A'/C_s$ for PtF_7^-, are more stable than the MCTP structures by 31.8 kcal/mol and 9 kcal/mol, respectively, at the CCSD(T)/aT-PP level. The bond distance between the external F atom and the F atom on the cluster is 2.05 Å in PtF_7^- and 2.07 Å in AuF_7^-, and the $M-F_{external}$ bond is 3.45 Å and 3.50 Å, respectively. The F−F bond distance is substantially longer than the F−F bond in F_2 of 1.412 Å[92] but is much shorter than the sum of the van der Waals radii[93] for two F atoms of 2.94 Å; the $M-F_{external}$ bond distance of ~3.5 Å in AuF_7^- is much longer than the average Au−F bond in AuF_6 of 1.895 Å at the B3LYP/aD-PP level. The M−F bond distance for the F atom bonded to the external F only lengthens by less than 0.05 Å. Thus this structure is quite unique. We optimized the same type of structures for the other metals in the series, and found that they are higher in energy than the classical structures by 87 kcal for the WF_7^- $^3A''/C_s$ structure, 54 kcal/mol for the ReF_7^- $^4A''/C_s$ structure, 25 kcal/mol for the OsF_7^- $^5A''/C_s$ structure, and 32 kcal/mol for the IrF_7^- $^2A'/C_s$ structure at the CCSD(T)/aT-PP level.

The average M−F bond distances in the classical structures of the MF_7^- series follow the same trend as in the MF_6 and MF_5 series, with M−F bonds of approximately the same length for M = W, Re, and Os and increasing for M = Ir, Pt, and Au. From WF_7^- to AuF_7^-, the average M−F bond distances are 1.901 Å, 1.900 Å, 1.902 Å, 1.921 Å, 1.922 Å, and 2.025 Å (excluding the long bond structures in PtF_7^- and AuF_7^-).

The FAs for the addition of F^- to form one of three classical structures are consistently between 70 and 85 kcal/mol. For M = W, Re, and Os, the spin state of the MF_7^- is the same as for MF_6 as expected from the simplest model. Addition of F^- to IrF_6 ($^4A_{1g}/O_h$) leads to a $^2B_1/C_{2v}$ classical structure for IrF_7^- and addition of F^- to PtF_6 ($^3A_{1g}/D_{4h}$) leads to a $^1A_1'/D_{5h}$ classical structure for PtF_7^-. Our calculated value of 77.9 kcal/mol (3.38 eV) for $FA(WF_6)$ is ~9 kcal/mol higher than the 69 kcal/mol (3.0 eV) estimated from ICR bracketing experiments.[8] Using more recent values[47] for the FAs (SiF_4 (77.4) < WF_6 < BF_3 (82.1)) we obtain excellent agreement between experiment and theory. The lowest value is for IrF_6 with a FA of ~70 kcal/mol.

The FAs for the formation of the non-classical structures show a much greater variation with the metal, from near 0 for WF_6 to values of 84.4 and 111.5 kcal/mol, respectively, for PtF_6 and AuF_6; the non-classical structures are the more stable than the classical ones for the latter two MF_6 (Table 9). The FAs for the non-classical structures increase with an increase in the atomic number of the central metal atom. The spin orbit effects are not large for the fluoride affinities.

Examination of the calculated spin density and charges in the classical structures for MF_7^- shows that the negative charge is distributed relatively evenly over the F atoms in the cluster, and the spin is predominantly localized on the central metal atom. However, in the non-classical structure, one spin is localized on the external F atom with the remaining spin localized mostly on the metal atom with some spin on the F adjacent to the external F atom. The charge distribution also differs from the classical structures with the external F carrying much less negative charge. Thus, the non-classical structure is best described as an F atom bonded to MF_6^-.

We can estimate the bond energy between the F atom and the MF_6^- from the following thermodynamic cycle,

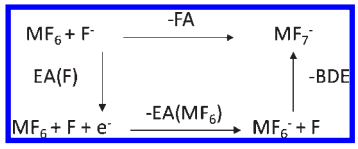

which uses available thermodynamic values to calculate the BDE of the process $MF_7^- \rightarrow MF_6^- + F$ given by BDE = EA(F) − EA(MF_6) + FA. The fluoride and electron affinities of MF_6 are available from our calculations, and the experimental electron affinity[28] of F is 3.4012 eV (78.43 kcal/mol). The results in Table 9 show that the MF_6^-−F BDE decreases from 84 kcal/mol for W to 10 kcal/mol for Ir for the classical MF_7^- structures, consistent with the increase in the MF_6 electron affinity. For PtF_7^-, the BDE is essentially zero, consistent with the formation of the F atom very weakly associated to PtF_6^-. A similar BDE of only 3.4 kcal/mol is predicted for AuF_7^-. Thus, when the electron affinity of MF_6 becomes large enough, the MF_6 will accept an F^- which then undergoes an electron transfer to MF_6 leaving a weak complex of an F atom with the MF_6^- anion. Thus, PtF_6 can oxidize F^- to $F^{\cdot}$, which explains its unusually high oxidizing power and reactivity. This is in excellent agreement with the previous experimental observations that PtF_6 can oxidize ClF_5 to ClF_6^+,[94,95] NF_3 to NF_4^+,[96] and Xe to XeF^+.[3,4] The mechanism of the NF_4^+ formation by different methods has been investigated in great detail[96] and been shown to involve the generation of F atoms as the crucial first step.

It is reasonable to assume that, in the reaction of Xe with PtF_6, the formation of an F atom is also the crucial first step. This would lead to the formation of a XeF radical which then gets oxidized by PtF_6 to give $XeF^+PtF_6^-$ and, by reacting with PtF_5, can yield $XeF^+Pt_2F_{11}^-$. This mechanism would account for the failure to observe experimentally any direct or indirect evidence for the formation of $Xe^+PtF_6^-$, with $XeF^+PtF_6^-$ and $XeF^+Pt_2F_{11}^-$ being the only observable products. On the basis of their extraordinarily high electron affinities, the third row transition metal hexafluorides ReF_6 (EA = 4.61 eV) through AuF_6 (EA = 8.20 eV)

(92) Huber, K. P.; Herzberg, G. *Molecular Spectra and Molecular Structure. IV. Constants of Diatomic Molecules*; Van Nostrand Reinhold Co.: New York, 1979.
(93) Bondi, A. *J. Phys. Chem.* **1964**, *68*, 441. Mantina, M.; Chamberlain, A. C.; Valero, R.; Cramer, C. J.; Truhlar, D. G. *J. Phys. Chem. A* **2009**, *113*, 5806.
(94) Christe, K. O. *Inorg. Nucl. Chem. Lett.* **1972**, *8*, 741.
(95) Roberto, F. Q. *Inorg. Nucl. Chem. Lett.* **1972**, *8*, 737.
(96) Christe, K. O.; Wilson, W. W.; Wilson, R. D. *Inorg. Chem.* **1984**, *23*, 2058.

Table 10. Calculated Fluoride Affinities for MF_5 (in kcal/mol)

	state/sym							
M	MF_5	MF_6^-	ΔFA_{CBS}[a]	ΔE_{ZPE}	ΔE_{CV}[b]	ΔE_{rel}[c]	ΔE_{SO}[d]	FA
W	$^2A_2/C_{2v}$	$^2B_{2g}/D_{4h}$	112.5	−0.70[e]	0.33	−0.06	0.78	112.9
Re	$^3A_1'/D_{3h}$	$^3A_{1g}/D_{4h}$	114.9	−1.69[f]	0.89	−0.27	2.59	116.4
Os	$^4B_1/C_{4v}$	$^4A_{1g}/O_h$	133.4	−1.64[f]	0.91	−0.44	−0.27	132.0
Ir	$^5B_1/C_{4v}$	$^3A_{1g}/D_{4h}$	137.8	−1.12[g]	0.05	1.13	−3.25	134.6
Pt	$^2B_1/C_{4v}$	$^2B_{2g}/D_{4h}$	129.3	−2.19[g]	1.00	−0.22	2.87	130.7
Au	$^1A_1/C_{4v}$	$^1A_{1g}/O_h$	140.3	−1.94[g]	1.09	0.37	−3.27	136.6

[a] Extrapolated using the mixed Gaussian/exponential formula. [b] CCSD(T)/awCVTZ. [c] See eq 1. [d] SO correction at the ADF ZORA BLYP/TZ2P level. [e] ADF ZORA SO BLYP/TZ2P. [f] BP86/aD-PP. [g] B3LYP/aT-PP.

definitely fall in the category of "superhalogens", a term created in 1981 by Gutsev and Boldyrev for compounds having electron affinities exceeding those of the halogens (3.0−3.6 eV).[97] Its high EA of 8.20 eV makes AuF_6 one of the ultimate superhalogens.

The predicted F^- affinity of AuF_6, leading to the formation of an F radical, is 111.8 kcal/mol and is only about 10 kcal/mol below that of SbF_5.[47] This would make AuF_6 not only a very powerful oxidizer but also a very strong Lewis acid. Because of their lower electron affinities, WF_6, ReF_6, OsF_6, and IrF_6 favor the classical MF_7^- structures with M−F bonds and do not react in the non-classical fashion.

Given the available results, it is also possible to calculate the MF_5 fluoride affinities ($MF_5 + F^- \rightarrow MF_6^-$). The resulting values calculated at the CCSD(T)/CBS level with ZPE, core−valence and scalar relativistic corrections are given in Table 10. The MF_5 fluoride affinities calculated as a function of the basis sets are given as Supporting Information. The MF_5 FAs increase from $FA(WF_5)$ = 113.0 to $FA(AuF_5)$ = 136.6 kcal/mol following the trends in the electron affinities. Our calculated value of 110.4 kcal/mol for $FA(WF_5)$ is in good agreement with the experimental value of 107.6 kcal/mol.[98] The DFT calculated value for $FA(AuF_5)$ = 141.2 kcal/mol[99] is in good agreement with our CCSD(T) value. Christe et al.[47] have used fluoride ion affinities to establish a quantitative Lewis acidity scale. The strongest Lewis acid on the list, SbF_5, has a fluoride affinity of 120.3 kcal/mol, lower than those of OsF_5, IrF_5, PtF_5, and AuF_5. WF_5 and ReF_5 with fluoride affinities of 112.1 and 115.0 kcal/mol, respectively, are comparable to strong Lewis acids such as AlF_3 and $AlCl_3$. The FAs of MF_5 are much larger by 35 to 58 kcal/mol than the FAs of the corresponding MF_6 molecules. This would be expected as going from a C_{4v} or D_{3h} structure for MF_5 to an approximate or actual octahedral structure for MF_6^- would have less steric crowding than going from an octahedral structure for MF_6 to the various structures for MF_7^-.

Performance of Density Functional Theory. There is substantial interest in the performance of different DFT exchange-correlation functionals in predicting the thermodynamic properties of transition metal complexes. Calculated EAs for a selection of functionals, M−F bond dissociation energies, calculated MF_5 FAs, and calculated MF_6 FAs are given in the Supporting Information. The average deviations of these properties calculated with a selection of functionals from the CCSD(T)/CBS values with all corrections except for spin orbit are given in Table 11. In general, the electron affinity differences between the CCSD(T) and DFT values are larger for the later transition metal fluorides than for the earlier ones. The largest differences are found for the LSDA functional SVWN5 with an average deviation of 26.0 kcal/mol. The GGA functionals perform somewhat better than SVWN5, but the differences from the CCSD(T) values are still quite large with average deviations of 15 to 20 kcal/mol. The hybrid functionals B3LYP, mPW1PW91, and PBE1 give the best performances with average deviations of 6−7 kcal/mol, but other hybrid functionals do not perform any better than the GGA functionals. Our B3LYP and BP86 calculated values of 7.96 and 7.10 eV for the electron affinity of AuF_6 are in excellent agreement with those of 8.06 and 7.10 eV, respectively, calculated by Riedel and Kaupp,[43] but the B3LYP values are ∼0.2 eV lower than our CCSD(T) value. For the M−F adiabatic BDEs of MF_6, the GGA functionals predict BDEs that are too large by up to 20 kcal/mol as compared to the CCSD(T) results. The hybrid functionals B3LYP, mPW91, and PBE1 predict M−F BDEs within 3 kcal/mol of the CCSD(T) results. For the MF_5 fluoride affinities, the GGA functionals predict values that are 8 to 19 kcal/mol smaller than the CCSD(T) values. Surprisingly, the best overall average agreement for the MF_5 FAs with the CCSD(T) values is with the local SVWN5 functional. The hybrid functionals also predict average values smaller than the CCSD(T) results by 3 to 16 kcal/mol. For the MF_6 fluoride affinities, the GGA functionals again show the largest differences on average with respect to the CCSD(T) values with average differences from 8 to 19 kcal/mol. The largest differences with these functionals are for $FA(PtF_6)$ and AuF_6, where the lowest energy MF_7^- structure is the non-classical structure. All hybrid functionals, except for O3LYP, predict average FAs within 2 to 6 kcal/mol with respect to the CCSD(T) values. The local SVWN5 performs well for the classical MF_7^- structures but does not for the non-classical structures for PtF_7^- and AuF_7^-.

Table 11. Average Deviations of the MF_6 Electron Affinities, MF_5 and MF_6 Fluoride Affinities, and First Adiabatic M−F Bond Dissociation Energies from the CCSD(T) Calculated Values (in kcal/mol)

functional	references	EA(MF_6)	FA(MF_5)	FA(MF_6)	M−F BDE
SVWN5	48, 49	23.9	0.5	3.8	−41.1
BLYP	24, 50	20.6	16.3	15.7	−11.2
BP86	50, 51	20.7	14.3	13.9	−15.4
PW91	52, 53	20.5	8.2	8.1	−8.4
PBE	54, 55	22.6	13.1	12.7	−16.3
TPSS	56	21.9	10.2	9.7	−12.3
HCTH	57	15.8	19.0	19.2	−7.9
B3LYP	23, 24	4.5	8.6	6.4	1.2
mPW1	52, 53, 58	4.5	5.4	4.0	3.0
PBE1	54	6.0	5.2	3.3	1.8
O3LYP	24, 59,	13.7	16.4	14.5	−38.8
TPSSh	56	21.8	2.8	2.0	−34.0

Conclusions

High level coupled cluster CCSD(T) calculations, extrapolated to the complete basis set limit, were used to evaluate

(97) Gutsev, G. L.; Boldyrev, A. I. *Chem. Phys.* **1981**, *56*, 277.
(98) Burgess, J.; Peacock, R. D. *J. Fluorine Chem.* **1977**, *10*, 479.
(99) Hwang, I. C.; Seppelt, K. *Angew. Chem., Int. Ed.* **2001**, *40*, 19.

reliable, self-consistent thermochemical data sets for the third row transition metal hexafluorides. For MF_6 and MF_6^-, the Jahn−Teller distorted D_{4h} and D_{3d} structures where possible are very close in energy with an undistorted O_h structure about 1.0 kcal/mol higher in energy. Thus, the MF_6 molecules are highly fluxional about the conical intersection and will exhibit an O_h geometry under most experimental conditions.

The electron affinities are direct measures for the oxidizer strengths of these hexafluorides, and their oxidizing power increases monotonically from WF_6 to AuF_6, with PtF_6 and AuF_6 being extremely powerful oxidizers. The inclusion of spin orbit corrections was very important to obtain the correct qualitative order for the electron affinities. A wide range of DFT exchange-correlation functionals were also evaluated and only the B3LYP, mPW1PW91, and PBE1 functionals were found to approximate the coupled cluster values.

On the basis of their calculated fluoride ion affinities, the corresponding pentafluorides are extremely strong Lewis acids, with OsF_5, IrF_5, PtF_5, and AuF_5 significantly exceeding the acidity of SbF_5.[47] A calculation of the minimum energy structures of the MF_6^- anions without or with (except for PtF_6^-) spin orbit corrections revealed that WF_6^-, ReF_6^-, IrF_6^-, and PtF_6^- are all distorted from O_h to D_{4h} symmetry with concomitant splittings of the degenerate vibrational modes which, in the case of the scissoring deformation, can lead to interesting frequency reversals depending on whether the axial or the equatorial bonds are shorter.

The calculation of the minimum energy structures for the corresponding MF_7^- anions resulted in a very important discovery. Whereas the hexafluorides ranging from WF_6 through IrF_6 form the expected classical MF_7^- anions with M−F bonds, PtF_7^- and AuF_7^- form non-classical anions with a very weak external F−F bond between an MF_6^- fragment and a fluorine atom. Therefore, these two anions are text book examples for "superhalogens" and can serve as F atom sources under very mild conditions. This ability of PtF_6 to generate, in the presence of fluoride anions, F atoms can explain its ability to convert NF_3 to NF_4^+, ClF_5 to ClF_6^+, and Xe to XeF^+. It also explains the failure of Bartlett's search for $XePtF_6$ and the observation of XeF^+ salts as the only reaction products of the PtF_6/Xe reaction.[3,4] The crucial first step appears to be the formation of a XeF radical which then is oxidized by PtF_6 to give $XeF^+PtF_6^-$.

Acknowledgment. This work was supported by the Chemical Sciences, Geosciences and Biosciences Division, Office of Basic Energy Sciences, U.S. Department of Energy (DOE) under Grant DE-FG02-03ER15481 (catalysis center program). D.A.D. also thanks the Robert Ramsay Chair Fund of The University of Alabama for support. Part of this work was performed at the W. R. Wiley Environmental Molecular Sciences Laboratory, a national scientific user facility sponsored by DOE's Office of Biological and Environmental Research and located at Pacific Northwest National Laboratory, operated for the DOE by Battelle. K.O.C. is indebted to the Air Force Office of Scientific Research, the Office of Naval Reesearch, the National Science Foundation, and the Defense Threat Reduction Agency for financial support.

Supporting Information Available: Experimental atomic heats of formation in kcal/mol, benchmarked DFT exchange-correlation functional, relative energy differences between the D_{4h} and D_{3d} MF_6 structures, $EA(MF_6)$, $FA(MF_5)$, $FA(MF_6)$, and first M−F BDEs calculated with various exchange-correlation functional, adiabatic electron affinities of MF_6, vertical electron detachment energies (VDE) of MF_6^-, and vertical electron attachment energies (VAE) of MF_6 in kcal/mol calculated at the CCSD(T)/aT-PP//CCSD(T)/aD-PP, B3LYP/aT-PP//B3LYP/aD-PP, and CCSD(T)/aT-DK//CCSD(T)/aT-PP levels, MF_6 MF_6^-, MF_5, and MF_7^- total electronic energies and vibrational frequencies at the DFT level with various exchange-correlation functionals and the aD-PP basis set, zero point energies (ZPE), CCSD(T) total energies as a function of basis set, core and valence energies at the CCSD(T)/aug-cc-pWCVTZ-PP level, and scalar relativistic energies at the CISD/aT-PP and CCSD(T)-DK/aug-cc-pVTZ-DK levels, T1 diagnostics. Energy differences in kcal/mol of D_{4h} vs O_h structures for the same spin state and singlet-triplet splitting energies for the D_{4h} structures. Optimized geometry parameters with different DFT functionals. Pseudopotential errors and scalar relativistic corrections for $EA(MF_6)$, 1st M−F BDEs, total atomization energies, $FA(MF_6)$, and $FA(MF_5)$. Electron affinities calculated at the ZORA and ZORA+SO levels. Mulliken charges, NBO charges, and spin densities for MF_6 and MF_6^- and figures for the spin densities. First M−F BDEs, $FA(MF_6)$, and $FA(MF_5)$ calculated at the DFT and CCSD(T) levels as a function of basis set. MF_5 optimized geometry at the B3LYP/aT-PP, BLYP/TZ2P scalar relativistic ZORA and ZORA plus spin orbit levels. Cartesian *xyz* coordinates for all molecules. This material is available free of charge via the Internet at http://pubs.acs.org.